GE Energy

Louis M. Quintana
Manager, Licensing

P.O. Box 780, M/C A-30
Wilmington, NC 28401
USA

T 910.675.6616
F 910.362.6616
Louis.Quintana@ge.com

GE Proprietary Information

MFN 05-029
April 8, 2005

U.S Nuclear Regulatory Commission
ATTN: Document Control Desk
Washington, D.C. 20555-0001

Attention: Herbert Berkow, Project Directorate IV
Program Manager

Subject: Responses to RAIs - **Methods Interim Process (TAC No. MC5780)**

In Reference 1, GE documented the proposed Methods Interim Process. The purpose of the Methods Interim Process is to allow the NRC to issue Safety Evaluations (SE) for the MELLLA + LTR and the future interim Methods LTR pending final NRC resolution of the NRC's request for additional information regarding GE's methods (Methods RAIs). GE committed in Reference 1 to provided the responses to those Methods RAIs required to judge the viability of, and ultimately approve, the Methods Interim Process. The first set of responses to the viability RAIs were issued in Reference 2.

The second set of responses to the viability RAIs were to be completed by April 8, 2005. Enclosure 1 contains all of the remaining responses to the viability RAIs. Non-proprietary versions of these responses are provided in Enclosure 2.

The affidavit contained in Enclosure 3 identifies that the information contained in Enclosure 1 has been handled and classified as proprietary to GE. GE hereby requests that the information Enclosure 1 be withheld from public disclosure in accordance with the provisions of 10 CFR 2.390 and 9.17.

D065

If you have any questions, please contact, Mike Lalor at (408) 925-2443 or myself.

Sincerely,

Louis M. Quintana

Louis M. Quintana
Manager, Licensing

Project No. 710

References:

1. MFN 05-005, Letter from George Stramback (GE) to NRC, March 25, 2005, *Methods Interim Process (TAC No. MC5780)*

2. MFN 05-022, Letter from George Stramback (GE) to NRC, March 31, 2005, *Responses to RAIs - Methods Interim Process (TAC No. MC5780)*

Enclosures:

1. GE Reponses to RAIs 5, 25, 26, 27, and 29 - Proprietary
2. GE Reponses to RAIs 5, 25, 26, 27, and 29 - Non-proprietary
3. Affidavit

cc: M Harding (GNF/Wilmington)
JF Harrison (GE/Wilmington)
CE Hinds (GE/Wilmington)
JF Klapproth (GE/Wilmington)
MA Lalor (GE/San Jose)
LM Quintana (GE/Wilmington)
PT Tran (GE/San Jose)
B. Moore (GE/Wilmington)
Alan Wang (NRC)
eDRF 0000-0009-3764

General Electric Company

AFFIDAVIT

I, Brad Erbes, state as follows:

(1) I am Manager, Technical Services, General Electric Company ("GE") and have been delegated the function of reviewing the information described in paragraph (2) which is sought to be withheld, and have been authorized to apply for its withholding.

(2) The information sought to be withheld is contained in Enclosure 1 to GE letter MFN 05-029, Louis Quintana to NRC, *Responses to RAIs - Methods Interim Process (TAC No. MC5780),* dated April 8, 2005. The proprietary information in Enclosure 1, *GE Reponses to RAIs 5, 25, 26, 27, and 29,* is delineated by a double underline inside double square brackets. Figures and large equation objects are identified with double square brackets before and after the object. In each case, the superscript notation{3} refers to Paragraph (3) of this affidavit, which provides the basis for the proprietary determination.

(3) In making this application for withholding of proprietary information of which it is the owner, GE relies upon the exemption from disclosure set forth in the Freedom of Information Act ("FOIA"), 5 USC Sec. 552(b)(4), and the Trade Secrets Act, 18 USC Sec. 1905, and NRC regulations 10 CFR 9.17(a)(4), and 2.390(a)(4) for "trade secrets" (Exemption 4). The material for which exemption from disclosure is here sought also qualify under the narrower definition of "trade secret", within the meanings assigned to those terms for purposes of FOIA Exemption 4 in, respectively, Critical Mass Energy Project v. Nuclear Regulatory Commission, 975F2d871 (DC Cir. 1992), and Public Citizen Health Research Group v. FDA, 704F2d1280 (DC Cir. 1983).

(4) Some examples of categories of information which fit into the definition of proprietary information are:

a. Information that discloses a process, method, or apparatus, including supporting data and analyses, where prevention of its use by General Electric's competitors without license from General Electric constitutes a competitive economic advantage over other companies;

b. Information which, if used by a competitor, would reduce his expenditure of resources or improve his competitive position in the design, manufacture, shipment, installation, assurance of quality, or licensing of a similar product;

c. Information which reveals aspects of past, present, or future General Electric customer-funded development plans and programs, resulting in potential products to General Electric;

d. Information which discloses patentable subject matter for which it may be desirable to obtain patent protection.

The information sought to be withheld is considered to be proprietary for the reasons set forth in paragraphs (4)a., and (4)b, above.

(5) To address 10 CFR 2.390 (b) (4), the information sought to be withheld is being submitted to NRC in confidence. The information is of a sort customarily held in confidence by GE, and is in fact so held. The information sought to be withheld has, to the best of my knowledge and belief, consistently been held in confidence by GE, no public disclosure has been made, and it is not available in public sources. All disclosures to third parties including any required transmittals to NRC, have been made, or must be made, pursuant to regulatory provisions or proprietary agreements which provide for maintenance of the information in confidence. Its initial designation as proprietary information, and the subsequent steps taken to prevent its unauthorized disclosure, are as set forth in paragraphs (6) and (7) following.

(6) Initial approval of proprietary treatment of a document is made by the manager of the originating component, the person most likely to be acquainted with the value and sensitivity of the information in relation to industry knowledge. Access to such documents within GE is limited on a "need to know" basis.

(7) The procedure for approval of external release of such a document typically requires review by the staff manager, project manager, principal scientist or other equivalent authority, by the manager of the cognizant marketing function (or his delegate), and by the Legal Operation, for technical content, competitive effect, and determination of the accuracy of the proprietary designation. Disclosures outside GE are limited to regulatory bodies, customers, and potential customers, and their agents, suppliers, and licensees, and others with a legitimate need for the information, and then only in accordance with appropriate regulatory provisions or proprietary agreements.

(8) The information identified in paragraph (2), above, is classified as proprietary because it contains detailed results and conclusions regarding GE Methods supporting evaluations of the safety-significant changes necessary to demonstrate the regulatory acceptability for the expanded power/flow range of MELLLA+ for a GE BWR, utilizing analytical models and methods, including computer codes, which GE has developed, obtained NRC approval of, and applied to perform evaluations of transient and accident events in the GE Boiling Water Reactor ("BWR"). The development and approval of these system, component, and thermal hydraulic models and computer codes was achieved at a significant cost to GE, on the order of several million dollars.

The development of the evaluation process along with the interpretation and application of the analytical results is derived from the extensive experience database that constitutes a major GE asset.

(9) Public disclosure of the information sought to be withheld is likely to cause substantial harm to GE's competitive position and foreclose or reduce the availability of profit-making opportunities. The information is part of GE's comprehensive BWR safety and technology base, and its commercial value extends beyond the original development cost. The value of the technology base goes beyond the extensive physical database and analytical methodology and includes development of the expertise to determine and apply the appropriate evaluation process. In addition, the technology base includes the value derived from providing analyses done with NRC-approved methods.

The research, development, engineering, analytical and NRC review costs comprise a substantial investment of time and money by GE.

The precise value of the expertise to devise an evaluation process and apply the correct analytical methodology is difficult to quantify, but it clearly is substantial.

GE's competitive advantage will be lost if its competitors are able to use the results of the GE experience to normalize or verify their own process or if they are able to claim an equivalent understanding by demonstrating that they can arrive at the same or similar conclusions.

The value of this information to GE would be lost if the information were disclosed to the public. Making such information available to competitors without their having been required to undertake a similar expenditure of resources would unfairly provide competitors with a windfall, and deprive GE of the opportunity to exercise its competitive advantage to seek an adequate return on its large investment in developing these very valuable analytical tools.

I declare under penalty of perjury that the foregoing affidavit and the matters stated therein are true and correct to the best of my knowledge, information, and belief.

Executed on this 8TH day of APRIL, 2005.

Brad Erbes
General Electric

ENCLOSURE 2

MFN 05-029

GE Responses to RAIs 5, 25,26, 27, and 29

Non-proprietary version

IMPORTANT NOTICE

This is a non-proprietary version of Enclosure 1 to MFN 05-029, which has the proprietary information removed. Portions of the enclosure that have been removed are indicated by an open and closed bracket as shown here [[ ]]

Non-proprietary version

NRC RAI RAI 5

Plant Data, PANAC comparisons, and Applicability to MELLLA+ Conditions. Several conclusions in the Methods Enclosure 3 state that the methods are adequate and that eigenvalue tracking per standard procedures will be used. Although, there are no EPU/MELLLA+ operational data, the adequacy of the GNF-A neutronic method must be substantiated through benchmark data or through data that is as close to the EPU/MELLLA+ conditions (e.g., high in channel void conditions 90% or greater). However, there is substantial data based on historical and current operation that are of interest. The following RAIs address benchmarking data needed to demonstrate the adequacy of the GNF-A method for the MELLLA+ conditions.

5-1 Section 2.1.2 states, [[

]]

5-2 Confirmation of Eigenvalues During MELLLA+ Implementation. In several sections, the conclusion states that "confirmation of thermal limits uncertainties (e.g., power distribution) should be executed for initial implementation of MELLLA+ strategy. Explain what is meant by this statement and how this confirmation is performed. As proposed, the eigenvalue tracking results and conclusions would be obtained during MELLLA+ operation after the staff's approval of plant-specific EPU/MELLLA+ application. State what process would be available to the staff for review or assessments of the eigenvalue benchmarking data after the approval of the plant-specific application. What process will this benchmarking data and the corresponding conclusions of the confirmation of the thermal limits uncertainties be provided to the staff for review and assessment?

5-3 Provide plant data and PANAC calculation results for core operating conditions that are as close to MELLLA+ operating conditions (120% power, 80% flow) as available. In this data provide:

a. Calculated radial and axial void fraction distributions. Provide plots and tabular data for comparisons with MELLLA+ conditions.

b. Measured TIP profiles and corresponding PANAC TIP predictions. Provide both plots and tabulation of the individual TIP readings and PANAC predictions and compute RMS deviations. The tabulation provides a better means to show the difference between the individual four bundle TIP reading and the associated PANAC results.

5-4 Provide the PANAC calculated data for the same parameters as requested in RAI 5-3 for a core with MELLLA+ conditions for comparison with existing plant data and

corresponding PANAC predictions. Provide in plots and tabular form to be consistent with results provided in the response to RAI 5-3.

5-5 Provide a discussion of how the core follow data is used to benchmark the GNF-A analytical methods. Explain the important plant instrumentation readings that are obtained from the licensees to simulate the core response using "offline" PANAC calculations. Discuss how the data is compared to the core monitoring system predictions. Provide tabulated data (shown during the audit), comparing the PANAC calculations and the plant's core monitoring system calculational results (e.g., core thermal power, exposure, core flow, thermal limits calculations) for the given cycle data points. Use Brunswick Units 1 and 2 core follow data and a high density BWR plant operating with the highest core void conditions. Include core follow data for operation in the high power/low flow offrated conditions for a high density plant. This is of interest in order to access the GNF-A code system's accuracy under high void offrated conditions as close to the EPU/MELLLA+ condition.

GE Response

Response to RAI 5-1

[[

]]

Response to RAI 5-2

Once a core has operated within the MELLLA+ domain, the following are to be evaluated:

- Hot critical eigenvalue
- Cold critical eigenvalue
- Nodal power distribution
- Bundle power distribution
- Rod-to-rod power distribution
- The core flow and pressure drop uncertainty
- The MIP criterion.

For the evaluation of eigenvalue behavior, see Response 25. The evaluation of nodal and bundle power distributions are conducted via comparison between measured and calculated TIP readings. Rod-to-rod power distributions can be evaluated by comparison between TGBLA and MCNP for the lattice designs present. The plant uncertainties are confirmed using plant data. The MIP criterion is evaluated during the SLMCPR generation process to determine if the core & fuel design selected for operation is expected to produce a plant response substantially outside of prior experience.

When this operational data has been analyzed, a revision to the Methods LTR will be provided to the staff for further review. Additionally, much of this same information will be provided when Licensed Topical Reports for GE approved methodologies are revised per the staff's request.

Response to RAI 5-3
The information regarding operational data for high power/flow ratio situations is provided in both graphical and tabular form in responses to RAIs 27 and 29. Additionally, the responses to RAIs 25 and 26 are pertinent to the data requested.

Response to RAI 5-4
The Methods Interim Process (Reference 5-1) definition includes [[

]] Therefore, this type of information would be submitted on a plant specific application for those plants that elected to utilize the Methods Interim Process.

Response to RAI 5-5
Plant core follow data is used to benchmark GNF-A methods as demonstrated in NEDC-30130P-A which includes evaluation of hot eigenvalues, cold eigenvalues, and TIPs. For this MELLLA+ analysis, a comprehensive evaluation of the same spirit is included as a part of RAI 25.

Additionally, comparison of core monitoring thermal limits and core follow thermal limits is available in Tables 5-2 through 5-10. The statistical summary is shown in Table 5-1. For each cycle, the thermal limits of the official core follow calculations are compared with the core monitoring output. It should be noted that for Plant B Cycle 9 and Plant E Cycle 9, the core monitor and off-line core following are performed with PANAC10. Additionally, the thermal-mechanical limits for these cycles are protected using composite MAPLHGR limits as defined Amendment 19 of GESTAR-II. Therefore, the MFLPD for these cycles is not relevant and is omitted from the tables for these cycles, as well as the statistical rollup for MFLPD.

For Plant D, the off-line core following is PANAC10 while the core monitor is a non-GE core monitoring system.

As demonstrated in Figures 5-1, 5-2, and 5-3, the data shows no significant trending versus core power/flow ratio, defined as core power (MWt) divided by total core flow (Mlbm/hr). [This indicator is also used in the response to RAI 25 in order to capture changes in the operating domain or region of the core power/flow map.] The overall average and standard deviation are consistent with methods requirements for nuclear design. Any specific trending is minor. Specific differences for a given cycle are procedurally reviewed prior to each new cycle of operation.

A similar review was conducted by GE in 2002 and presented to the NRC. This information, where PANAC10 and PANAC11 were specifically separated, was formally transmitted to the NRC as a part of Reference 5-2. They are repeated here in Figure 5-4 for additional information. Comparison of this historical analysis to the present indicates that the results are very similar and end up with statistical behavior between the PANAC10 and PANAC11 specific distributions, as expected.

Non-proprietary version

Table 5-1 Statistical Summary of Thermal Margin Prediction (Offline – Core Monitoring)

	DELTA MFLPD	DELTA MAPRAT	DELTA MFLCPR
AVG	[[		
STDEV			]]

Non-proprietary version

Table 5-2 Plant A, Cycle 18 Thermal Limits Comparison

N	CYCEXP	RP	WCT	PANAC MFLPD	PANAC MAPRAT	PANAC MFLCPR	CM MFLPD	CM MAPRAT	CM MFLCPR
1	19.07	544.00	27.08	[[					
2	32.26	969.00	27.30						
3	169.47	1241.00	38.81						
4	205.11	1317.00	31.13						
5	341.75	1660.00	48.07						
6	366.13	768.00	28.33						
7	383.82	1333.00	32.15						
8	406.48	1658.00	47.53						
9	723.83	1657.00	47.49						
10	753.10	880.00	28.15						
11	775.72	1658.00	46.51						
12	1049.26	1656.00	46.67						
13	1163.30	1655.00	45.67						
14	1207.88	1655.00	45.75						
15	1246.74	1417.00	35.37						
16	1260.82	804.00	27.56						
17	1283.49	1652.00	47.90						
18	1443.08	1655.00	47.07						
19	1610.91	1658.00	46.33						
20	1637.19	1384.00	34.87						
21	1659.87	1655.00	47.92						
22	1910.73	1657.00	46.67						
23	2138.76	1658.00	46.29						
24	2344.02	1657.00	45.64						
25	2663.26	1658.00	45.86						
26	2731.68	1657.00	45.31						
27	3044.61	1657.00	45.71						
28	3057.86	751.00	37.54						
29	3071.82	797.00	33.50						
30	3094.32	1581.00	41.94						
31	3208.21	1654.00	47.13						
32	3367.70	1658.00	46.99						
33	3411.50	1654.00	46.83						
34	3427.40	1157.00	36.15						
35	3447.35	1501.00	36.82						
36	3469.08	1599.00	42.02						
37	3512.75	1656.00	45.28						

Non-proprietary version

Table 5-2 Plant A, Cycle 18 Thermal Limits Comparison

N	CYCEXP	RP	WCT	PANAC MFLPD	PANAC MAPRAT	PANAC MFLCPR	CM MFLPD	CM MAPRAT	CM MFLCPR
38	3548.56	1562.00	39.84						
39	3571.44	1656.00	45.00						
40	3595.21	1717.00	46.27						
41	3692.02	1760.00	46.84						
42	3962.59	1789.00	47.02						
43	4184.18	1790.00	46.17						
44	4504.30	1780.00	46.32						
45	4627.43	1791.00	46.83						
46	4644.69	955.00	30.03						
47	4667.83	1786.00	47.96						
48	4959.86	1769.00	48.29						
49	5252.02	1770.00	47.34						
50	5264.14	846.00	24.40						
51	5281.94	1497.00	35.67						
52	5306.17	1769.00	45.68						
53	5573.94	1768.00	46.77						
54	5768.73	1768.00	46.10						
55	5939.16	1770.00	45.60						
56	6129.19	1768.00	47.23						
57	6148.73	1420.00	39.47						
58	6172.36	1731.00	43.40						
59	6369.31	1788.00	46.61						
60	6566.21	1788.00	46.26						
61	6910.95	1788.00	47.31						
62	7156.70	1789.00	46.42						
63	7178.40	1789.00	46.33						
64	7399.96	1792.00	47.33						
65	7621.56	1789.00	46.48						
66	7818.53	1790.00	45.95						
67	7847.05	1791.00	47.33						
68	7875.36	1214.00	31.79						
69	7898.28	1768.00	44.17						
70	7922.88	1789.00	46.98						
71	8144.47	1788.00	46.18						
72	8415.33	1791.00	45.91						
73	8636.51	1786.00	47.13						
74	8858.10	1789.00	46.86						
75	9103.54	1791.00	46.35						
76	9125.01	1772.00	48.14						

Non-proprietary version

Table 5-2 Plant A, Cycle 18 Thermal Limits Comparison

N	CYCEXP	RP	WCT	PANAC MFLPD	PANAC MAPRAT	PANAC MFLCPR	CM MFLPD	CM MAPRAT	CM MFLCPR
77	9149.58	1787.00	47.38						
78	9420.38	1789.00	46.68						
79	9678.82	1792.00	46.69						
80	9692.61	753.00	29.59						
81	9716.17	1749.00	44.67						
82	9740.74	1788.00	46.64						
83	10060.79	1788.00	46.03						
84	10089.00	1739.00	46.36						
85	10111.74	1064.00	31.87						
86	10129.10	1255.00	44.04						
87	10180.09	1240.00	29.17						
88	10198.26	1281.00	34.84						
89	10222.65	1790.00	46.12						
90	10345.66	1789.00	47.67						
91	10616.45	1788.00	47.04						
92	10788.76	1788.00	46.12						
93	11010.26	1789.00	46.74						
94	11025.84	1074.00	33.58						
95	11042.68	1230.00	33.26						
96	11066.76	1748.00	44.04						
97	11263.69	1792.00	47.56						
98	11485.27	1788.00	46.06						
99	11706.87	1789.00	47.17						
100	11903.80	1791.00	46.12						
101	12125.40	1789.00	47.45						
102	12346.90	1789.00	45.90						
103	12568.50	1790.00	47.56						
104	12691.60	1791.00	47.05						
105	12912.70	1790.00	47.54						
106	13232.70	1792.00	47.04						
107	13251.50	1347.00	36.18						
108	13276.00	1792.00	46.30						
109	13374.50	1791.00	47.87						
110	13575.20	1792.00	46.89						
111	13592.19	1135.00	26.28						
112	13615.56	1665.00	48.59						
113	13639.88	1787.00	47.87						
114	13886.01	1789.00	45.76						
115	13984.48	1789.00	47.42						

Non-proprietary version

Table 5-2 Plant A, Cycle 18 Thermal Limits Comparison

N	CYCEXP	RP	WCT	PANAC MFLPD	PANAC MAPRAT	PANAC MFLCPR	CM MFLPD	CM MAPRAT	CM MFLCPR
116	14082.94	1786.00	47.47						
117	14156.79	1791.00	48.09						
118	14230.63	1789.00	48.08						
119	14304.47	1790.00	48.34						
120	14353.71	1788.00	48.16						
121	14445.74	1789.00	48.18						]]

Non-proprietary version

Table 5-3 Plant A, Cycle 19 Thermal Limits Comparison

N	CYCEXP	RP	WCT	PANAC MFLPD	PANAC MAPRAT	PANAC MFLCPR	CM MFLPD	CM MAPRAT	CM MFLCPR
1	19.18	997.00	31.93	[[					
2	43.04	1737.00	43.49						
3	67.57	1787.00	47.39						
4	190.47	1789.00	47.28						
5	239.64	1790.00	46.48						
6	510.12	1790.00	47.18						
7	854.37	1791.00	46.69						
8	1100.25	1790.00	45.72						
9	1173.95	1791.00	45.27						
10	1468.88	1791.00	46.35						
11	1763.87	1786.00	45.58						
12	2058.89	1790.00	46.44						
13	2132.66	1790.00	46.22						
14	2378.23	1789.00	46.02						
15	2400.54	1783.00	46.79						
16	2425.09	1789.00	47.75						
17	2498.84	1789.00	46.68						
18	2720.14	1789.00	46.43						
19	3035.95	1788.00	45.76						
20	3060.38	1787.00	45.67						
21	3158.71	1792.00	47.40						
22	3379.98	1790.00	47.24						
23	3724.21	1787.00	46.74						
24	4043.84	1792.00	46.12						
25	4191.37	1791.00	45.75						
26	4363.48	1789.00	45.51						
27	4434.32	1789.00	47.32						
28	4505.56	1792.00	47.94						
29	4801.28	1789.00	47.60						
30	4869.83	508.00	25.57						
31	5184.95	1792.00	47.89						
32	5406.20	1790.00	48.09						
33	5524.65	1788.00	46.29						
34	5793.33	1788.00	47.31						
35	6014.63	1793.00	47.06						
36	6260.54	1789.00	46.23						
37	6506.52	1789.00	45.76						

Non-proprietary version

Table 5-3 Plant A, Cycle 19 Thermal Limits Comparison

N	CYCEXP	RP	WCT	PANAC MFLPD	PANAC MAPRAT	PANAC MFLCPR	CM MFLPD	CM MAPRAT	CM MFLCPR
38	6727.89	1790.00	45.12						
39	6949.30	1791.00	46.74						
40	6969.49	1478.00	48.56						
41	6993.99	1791.00	46.05						
42	7215.37	1791.00	46.18						
43	7387.54	1792.00	46.00						
44	7608.93	1792.00	45.28						
45	7953.29	1791.00	47.06						
46	8125.50	1791.00	46.13						
47	8174.70	1791.00	45.97						
48	8193.89	1544.00	46.60						
49	8210.90	1023.00	26.39						
50	8235.36	1787.00	47.72						
51	8259.94	1789.00	47.58						
52	8278.03	944.00	26.69						
53	8302.29	1781.00	45.02						
54	8572.82	1787.00	47.40						
55	8843.39	1786.00	47.37						
56	9015.59	1790.00	46.98						
57	9138.58	1791.00	46.85						
58	9261.12	1790.00	46.72						
59	9307.89	1790.00	47.65						
60	9578.25	1794.00	45.88						
61	9824.20	1791.00	45.61						
62	10045.57	1788.00	45.63						
63	10340.72	1794.00	45.43						
64	10635.89	1794.00	45.51						
65	10931.02	1791.00	45.67						
66	11176.97	1793.00	45.98						
67	11422.89	1786.00	45.95						
68	11668.51	1788.00	46.89						
69	11763.69	1789.00	47.72						
70	11911.22	1788.00	46.95						
71	12009.56	1791.00	47.43						
72	12378.42	1792.00	47.09						
73	12525.93	1790.00	46.05						
74	12718.90	1791.00	47.15						
75	12756.90	1472.00	44.29						
76	12821.59	1490.00	39.31						

Non-proprietary version

Table 5-3 Plant A, Cycle 19 Thermal Limits Comparison

N	CYCEXP	RP	WCT	PANAC MFLPD	PANAC MAPRAT	PANAC MFLCPR	CM MFLPD	CM MAPRAT	CM MFLCPR
77	12842.13	1498.80	39.73						
78	12856.49	905.00	29.45						
79	12879.40	1545.00	36.13						
80	12903.92	1791.00	47.84						
81	12928.49	1789.00	47.46						
82	13248.08	1792.00	47.12						
83	13592.33	1794.00	47.00						
84	13764.33	1787.00	46.70						
85	13810.41	1792.00	48.26						
86	13859.58	1790.00	46.82						
87	14007.10	1795.00	47.81						
88	14277.63	1792.00	47.04						
89	14474.27	1784.00	46.81						
90	14621.80	1792.00	47.61						
91	14720.15	1789.00	47.72						
92	14769.31	1789.00	48.02						
93	14941.42	1788.00	47.27						
94	15088.61	1789.00	47.80						
95	15260.71	1791.00	47.33						
96	15482.01	1788.00	47.23						
97	15693.58	1768.00	48.83						]]

Non-proprietary version

Table 5-4 Plant B, Cycle 9 Thermal Limits Comparison

N	CYCEXP	RP	WCT	PANAC MAPRAT	PANAC MFLCPR	CM MAPRAT	CM MFLCPR
1	261.69	3760.00	103.97	[[			
2	392.69	3751.00	102.99				
3	540.80	3755.00	94.70				
4	792.08	3756.00	94.45				
5	930.11	2770.00	107.51				
6	1163.98	3755.00	100.26				
7	1416.58	3761.00	100.90				
8	1614.65	3753.00	98.22				
9	1891.15	3757.00	97.32				
10	2195.62	3756.00	93.97				
11	2499.26	3749.00	93.04				
12	2803.19	3761.00	91.99				
13	3107.13	3759.00	90.85				
14	3410.34	3749.00	88.24				
15	3486.24	3750.00	87.88				
16	3688.63	3757.00	89.57				
17	3865.74	3753.00	88.19				
18	4118.83	3754.00	88.56				
19	4393.85	3763.00	95.40				
20	4672.42	3758.00	94.00				
21	4976.32	3752.00	92.43				
22	5223.99	3754.00	92.36				
23	5348.47	3755.00	91.33				
24	5471.67	3195.00	95.05				
25	5688.96	3752.00	91.29				
26	5916.87	3758.00	91.43				
27	6059.69	3758.00	90.61				
28	6231.34	3748.00	100.78				
29	6356.54	3753.00	90.85				
30	6634.90	3756.00	90.64				
31	6919.06	3748.00	89.32				
32	7203.31	3752.00	101.37				
33	7481.62	3746.00	99.88				
34	7760.08	3759.00	98.90				
35	8037.19	3751.00	96.01				
36	8314.94	3762.00	93.49				
37	8491.94	3757.00	95.99				

Non-proprietary version

Table 5-4 Plant B, Cycle 9 Thermal Limits Comparison

N	CYCEXP	RP	WCT	PANAC MAPRAT	PANAC MFLCPR	CM MAPRAT	CM MFLCPR
38	8744.65	3755.00	97.36				
39	8972.33	3752.00	96.12				
40	9200.13	3755.00	94.12				
41	9326.39	3755.00	99.64				
42	9377.92	3748.00	102.32				
43	9583.04	3757.00	104.59				
44	9785.23	3747.00	103.53				
45	10057.69	3754.00	104.70				
46	10335.91	3759.00	104.38				
47	10563.46	3764.00	104.00				
48	10841.69	3763.00	103.31				
49	11120.07	3759.00	103.24				
50	11398.25	3761.00	103.64				
51	11695.55	3760.00	104.04				
52	11861.01	3752.00	99.46				
53	11998.08	3621.00	107.57				
54	12198.06	3726.00	107.78				
55	12372.59	3694.00	108.04				
56	12648.98	3760.00	99.93				
57	12927.22	3758.00	104.03				
58	13205.09	3752.00	106.38				
59	13255.55	3741.00	107.67				
60	13454.96	3756.00	94.50				
61	13708.11	3760.00	98.26				
62	13961.24	3730.00	101.01				
63	14237.24	3746.00	101.77				
64	14489.93	3739.00	107.47				
65	14763.69	3756.00	107.15				
66	14863.66	3714.00	107.95				
67	15034.43	3741.00	108.10				
68	15207.85	3655.00	108.67				
69	15342.44	3617.00	109.15				
70	15500.17	3166.00	108.68				
71	15627.24	3132.00	108.50				
72	15840.25	3193.00	103.76				
73	15990.45	3188.00	108.36				
74	16193.23	3117.00	109.21				]]

Non-proprietary version

Table 5-5 Plant B, Cycle 10 Thermal Limits Comparison

N	CYCEXP	RP	WCT	PANAC MFLPD	PANAC MAPRAT	PANAC MFLCPR	CM MFLPD	CM MAPRAT	CM MFLCPR
1	191.01	3752.00	104.86	[[					
2	267.23	3756.00	106.57						
3	444.96	3744.00	104.25						
4	521.16	3745.00	105.59						
5	800.48	3749.00	102.74						
6	1079.95	3749.00	102.57						
7	1359.42	3749.00	102.30						
8	1638.20	3758.00	101.14						
9	1883.99	3759.00	100.59						
10	2101.25	3757.00	100.36						
11	2253.07	3754.00	101.24						
12	2451.32	3750.00	99.51						
13	2515.04	3143.00	109.15						
14	2713.55	3751.00	95.89						
15	2822.36	3733.00	108.40						
16	3071.29	3750.00	97.00						
17	3322.81	3756.00	97.01						
18	3576.46	3758.00	97.09						
19	3829.77	3759.00	96.01						
20	4098.37	3757.00	96.43						
21	4178.58	3755.00	103.88						
22	4455.24	3754.00	98.81						
23	4733.80	3754.00	99.80						
24	5013.16	3753.00	98.31						
25	5156.27	3751.00	98.30						
26	5220.20	3595.00	108.21						
27	5495.19	3753.00	98.37						
28	5774.08	3751.00	97.89						
29	6053.51	3757.00	97.46						
30	6332.70	3760.00	97.01						
31	6612.04	3757.00	96.57						
32	6739.09	3758.00	94.91						
33	6804.45	3528.00	108.65						
34	7079.33	3754.00	100.81						
35	7358.64	3754.00	100.03						
36	7637.04	3756.00	99.08						
37	7915.93	3759.00	99.08						

Non-proprietary version

Table 5-5 Plant B, Cycle 10 Thermal Limits Comparison

N	CYCEXP	RP	WCT	PANAC MFLPD	PANAC MAPRAT	PANAC MFLCPR	CM MFLPD	CM MAPRAT	CM MFLCPR
38	8195.32	3751.00	97.79						
39	8449.34	3754.00	96.36						
40	8680.67	3759.00	95.96						
41	8953.97	3760.00	98.45						
42	9233.34	3752.00	98.67						
43	9512.33	3757.00	98.85						
44	9791.72	3758.00	98.62						
45	10071.07	3763.00	98.24						
46	10299.58	3760.00	97.56						
47	10528.19	3752.00	98.26						
48	10756.80	3757.00	98.61						
49	11010.32	3748.00	102.41						
50	11238.74	3755.00	103.54						
51	11467.28	3747.00	103.92						
52	11530.77	3748.00	99.10						
53	11630.58	3754.00	94.81						
54	11800.43	3750.00	99.53						
55	12079.80	3750.00	100.87						
56	12308.21	3748.00	103.13						
57	12512.36	3756.00	104.19						
58	12715.46	3756.00	107.50						
59	12992.27	3747.00	100.06						
60	13271.55	3741.00	103.76						
61	13576.18	3724.00	107.57						
62	13725.07	3751.00	103.37						
63	13923.32	3750.00	104.38						
64	14163.43	3568.00	108.46						
65	14391.74	3494.00	108.15						]]

Non-proprietary version

Table 5-6 Plant C, Cycle 30 Thermal Limits Comparison

N	CYCEXP	RP	WCT	PANAC MFLPD	PANAC MAPRAT	PANAC MFLCPR	CM MFLPD	CM MAPRAT	CM MFLCPR
1	28.22	553.00	22.80	[[					
2	51.25	1085.00	28.87						
3	121.68	1092.00	31.82						
4	285.84	1092.00	28.47						
5	426.66	1095.00	29.15						
6	682.10	1094.00	29.31						
7	940.49	1094.00	29.29						
8	1128.41	1092.00	28.96						
9	1434.20	1093.00	28.70						
10	1739.62	1094.00	28.54						
11	1853.68	1094.00	28.03						
12	2135.52	1094.00	27.89						
13	2252.96	1095.00	27.82						
14	2417.35	1094.00	27.85						
15	2534.80	1094.00	27.78						
16	2792.80	1095.00	27.71						
17	3050.94	1091.00	27.70						
18	3237.72	1096.00	27.90						
19	3331.62	1093.00	28.11						
20	3589.86	1097.00	28.32						
21	3715.89	1094.00	28.73						
22	3726.46	602.00	23.45						
23	3749.43	1091.00	32.36						
24	3771.81	1090.00	27.27						
25	3842.19	1094.00	26.29						
26	4006.37	1093.00	26.85						
27	4217.56	1093.00	27.16						
28	4381.54	1093.00	27.78						
29	4545.85	1093.00	28.44						
30	4710.15	1094.00	29.49						
31	4874.44	1095.00	29.88						
32	5037.76	1096.00	30.71						
33	5177.59	1096.00	31.49						
34	5338.56	1064.00	25.93						
35	5498.18	1057.00	25.92						
36	5638.93	1094.00	28.65						
37	5850.10	1093.00	30.02						

Non-proprietary version

Table 5-6 Plant C, Cycle 30 Thermal Limits Comparison

N	CYCEXP	RP	WCT	PANAC MFLPD	PANAC MAPRAT	PANAC MFLCPR	CM MFLPD	CM MAPRAT	CM MFLCPR
38	6061.20	1086.00	31.39						
39	6248.86	1094.00	31.39						
40	6344.99	1094.00	31.29						
41	6368.13	1088.00	28.86						
42	6390.56	985.00	28.87						
43	6412.42	1046.00	31.64						
44	6434.06	1058.00	32.02						
45	6454.85	849.00	23.16						
46	6475.04	932.00	25.89						
47	6558.57	949.00	27.22						
48	6693.98	1050.00	31.64						
49	6787.36	859.00	24.33						
50	6848.84	975.00	31.46						
51	6914.54	1048.00	32.64						
52	7068.27	1031.00	32.85						
53	7238.79	874.00	28.08						
54	7307.74	805.00	24.65						
55	7382.15	878.00	29.83						
56	7481.68	916.00	32.70						
57	7535.50	869.00	31.42						
58	7604.86	732.00	22.75						]]

Non-proprietary version

Table 5-7 Plant C

N	CYCEXP	RP	WCT	PANAC MFLPD	PANAC MAPRAT	PANAC MFLCPR	CM MFLPD	CM MAPRAT	CM MFLCPR
1	11.80	483.00	19.40	[[					
2	22.49	537.00	22.80						
3	36.81	663.00	19.31						
4	58.64	1092.00	26.40						
5	127.99	1093.00	27.90						
6	267.29	1096.00	28.51						
7	383.64	1095.00	28.78						
8	496.46	1031.00	26.00						
9	659.08	1097.00	29.09						
10	821.87	1096.00	29.09						
11	984.89	1093.00	29.02						
12	1147.89	1094.00	28.84						
13	1311.95	1097.00	28.84						
14	1474.95	1096.00	28.77						
15	1684.09	1095.00	27.86						
16	1893.66	1095.00	27.71						
17	2103.14	1096.00	27.56						
18	2311.05	1094.00	27.38						
19	2450.80	1095.00	27.31						
20	2613.86	1098.00	27.29						
21	2776.73	1094.00	27.13						
22	2939.64	1093.00	27.09						
23	3102.01	1092.00	27.60						
24	3264.96	1095.00	27.59						
25	3427.83	1095.00	27.60						
26	3590.68	1096.00	27.68						
27	3753.32	1095.00	27.86						
28	3916.13	1098.00	28.19						
29	4102.17	1094.00	28.32						
30	4286.02	1090.00	28.66						
31	4472.08	1095.00	28.98						
32	4611.41	1093.00	27.05						
33	4774.23	1093.00	27.22						
34	4935.85	1094.00	27.66						
35	5098.68	1095.00	28.16						
36	5261.19	1094.00	28.65						
37	5377.46	1094.00	29.46						
38	5585.81	1092.00	29.98						

Non-proprietary version

Table 5-7 Plant C

N	CYCEXP	RP	WCT	PANAC MFLPD	PANAC MAPRAT	PANAC MFLCPR	CM MFLPD	CM MAPRAT	CM MFLCPR
39	5702.12	1096.00	30.79						
40	5864.37	1092.00	26.77						
41	6073.73	1092.00	27.39						
42	6281.43	1094.00	28.44						
43	6490.72	1095.00	29.71						
44	6606.96	1095.00	30.87						
45	6723.22	1093.00	32.13						
46	6955.70	1094.00	31.94						
47	7160.47	1096.00	32.31						
48	7276.69	1089.90	32.43						
49	7391.51	1078.60	32.52						
50	7579.33	966.90	30.91						
51	7667.27	1035.50	32.65						
52	7825.45	900.70	28.73						]]

Non-proprietary version

Table 5-8 Plant D

N	CYCEXP	RP	WCT	PANAC MFLPD	PANAC MAPRAT	PANAC MFLCPR	CM MFLPD	CM MAPRAT	CM MFLCPR
1	349.87	2921.40	79.44	[[					
2	615.16	2920.50	79.40						
3	880.48	2924.60	78.06						
4	1145.81	2922.50	78.00						
5	1409.16	2927.60	80.17						
6	1727.54	2922.10	78.25						
7	1873.02	2923.70	79.91						
8	2111.79	2921.70	78.15						
9	2376.93	2918.40	76.69						
10	2642.03	2916.60	76.93						
11	2827.54	2921.30	78.67						
12	2969.29	2922.50	79.54						
13	3234.52	2914.50	78.60						
14	3403.00	2921.10	78.18						
15	3593.05	2920.40	79.33						
16	3858.26	2923.60	79.29						
17	4123.51	2917.70	78.27						
18	4388.74	2920.10	77.87						
19	4654.04	2926.20	76.92						
20	4849.98	2925.90	77.82						
21	5115.19	2922.20	78.38						
22	5247.85	2918.50	77.41						
23	5377.00	2920.50	78.60						
24	5642.28	2916.70	77.73						
25	5907.49	2924.60	79.48						
26	6172.76	2924.30	79.31						
27	6437.89	2919.80	78.06						
28	6728.40	2923.20	79.31						
29	6993.61	2925.70	78.63						]]

Non-proprietary version

Table 5-9 Plant E, Cycle 9 Thermal Limits Comparison

N	CYCEXP	RP	WCT	PANAC MAPRAT	PANAC MFLCPR	CM MAPRAT	CM MFLCPR
1	281.27	3215.00	78.19	[[			
2	579.35	3211.00	82.63				
3	888.96	3221.00	82.72				
4	1158.62	3279.00	82.97				
5	1378.09	3292.00	82.88				
6	1637.54	3282.00	79.16				
7	1851.06	3288.00	79.19				
8	2064.50	3282.00	80.97				
9	2331.60	3284.00	80.41				
10	2598.33	3286.00	80.13				
11	2891.95	3278.00	81.16				
12	3076.91	3261.00	78.66				
13	3336.79	3260.00	79.03				
14	3599.85	3232.00	78.25				
15	3914.44	3228.00	79.41				
16	4228.39	3214.00	78.25				
17	4540.20	3178.00	76.88				
18	4822.55	3169.00	77.97				
19	5106.23	3176.00	77.09				
20	5260.84	3168.00	76.56				
21	5415.38	3170.00	76.19				
22	5656.71	3170.00	76.97				
23	5955.78	3171.00	75.91				
24	6135.83	3167.00	77.09				
25	6315.89	3171.00	75.66				
26	6593.41	3163.00	80.56				
27	6850.99	3164.00	79.03				
28	7056.56	3163.00	77.81				
29	7236.61	3168.00	77.16				
30	7389.51	3172.00	78.06				
31	7543.78	3164.00	77.47				
32	7697.97	3165.00	76.16				
33	7903.42	3166.00	78.13				
34	8108.81	3157.00	76.41				
35	8339.86	3161.00	76.59				
36	8468.29	3162.00	77.44				
37	8621.00	3159.00	77.09				

Non-proprietary version

Table 5-9 Plant E, Cycle 9 Thermal Limits Comparison

N	CYCEXP	RP	WCT	PANAC MAPRAT	PANAC MFLCPR	CM MAPRAT	CM MFLCPR
38	8757.27	3156.00	78.66				
39	8936.77	3158.00	78.47				
40	9013.73	3159.00	78.56				
41	9142.13	3166.00	78.56				
42	9296.28	3173.00	77.91				
43	9476.57	3172.00	77.63				
44	9624.08	3171.00	78.72				
45	9833.08	3230.00	79.16				
46	10016.09	3214.00	78.75				
47	10199.38	3226.00	79.16				
48	10278.04	3236.00	80.16				
49	10540.82	3239.00	80.53				
50	10777.66	3228.00	80.41				
51	10935.93	3245.00	81.94				
52	11120.22	3242.00	80.31				
53	11304.63	3237.00	80.56				
54	11489.20	3252.00	80.09				
55	11621.02	3245.00	78.94				
56	11699.95	3244.00	81.44				
57	11858.13	3246.00	80.44				
58	12069.42	3254.00	80.16				
59	12227.88	3252.00	82.06				
60	12306.81	3235.00	78.84				
61	12438.02	3231.00	81.38				
62	12485.24	3157.00	81.88				
63	12768.11	3170.00	79.41				
64	12947.69	3164.00	78.66				
65	13126.98	3152.00	78.13				
66	13306.22	3151.00	78.22				
67	13485.89	3153.00	80.50				
68	13743.26	3155.00	79.94				
69	13831.22	3225.00	83.78				
70	14144.82	3226.00	83.44				
71	14426.98	3182.00	86.72				
72	14620.81	3102.00	87.06				
73	14836.51	3041.00	87.41				
74	14934.45	2994.00	87.72				
75	15204.23	3042.00	87.81				
76	15485.38	2926.00	86.97				

Non-proprietary version

Table 5-9 Plant E, Cycle 9 Thermal Limits Comparison

N	CYCEXP	RP	WCT	PANAC MAPRAT	PANAC MFLCPR	CM MAPRAT	CM MFLCPR
77	15761.77	2827.00	88.75				
78	15981.40	2712.00	89.25				]]

Non-proprietary version

Table 5-10 Plant E, Cycle 10 Thermal Limits Comparison

N	CYCEXP	RP	WCT	PANAC MFLPD	PANAC MAPRAT	PANAC MFLCPR	CM MFLPD	CM MAPRAT	CM MFLCPR
1	174.07	3215.30	80.66	[[					
2	357.79	3227.50	84.91						
3	541.67	3225.60	83.00						
4	614.91	3225.40	82.75						
5	907.12	3218.30	80.78						
6	1194.86	3219.80	80.31						
7	1486.05	3279.30	82.53						
8	1779.71	3288.20	82.16						
9	1837.28	1668.70	63.34						
10	2078.90	3300.90	80.22						
11	2319.92	3293.60	80.94						
12	2561.44	3311.00	81.34						
13	2830.29	3300.30	79.41						
14	2910.81	3303.00	79.81						
15	3125.56	3303.30	79.53						
16	3340.80	3308.80	80.03						
17	3385.63	3314.50	82.03						
18	3648.16	3309.70	81.44						
19	3917.25	3309.20	82.03						
20	4185.95	3313.00	81.59						
21	4454.79	3314.70	80.88						
22	4562.31	3309.40	81.09						
23	4589.14	3298.70	82.41						
24	4640.39	3311.80	83.81						
25	4855.56	3301.80	82.66						
26	4909.24	3316.10	81.97						
27	5204.28	3308.30	83.41						
28	5472.07	3291.90	81.69						
29	5766.70	3297.90	82.38						
30	5819.00	3283.90	85.16						
31	6139.27	3282.30	82.91						
32	6460.36	3273.80	80.78						
33	6780.44	3292.60	81.13						
34	7100.63	3283.30	80.38						
35	7339.21	3288.50	81.50						
36	7579.67	3288.80	81.44						
37	7820.09	3294.00	80.63						

Non-proprietary version

Table 5-10 Plant E, Cycle 10 Thermal Limits Comparison

N	CYCEXP	RP	WCT	PANAC MFLPD	PANAC MAPRAT	PANAC MFLCPR	CM MFLPD	CM MAPRAT	CM MFLCPR
38	8033.81	3301.00	81.38						
39	8266.38	3209.70	82.25						
40	8543.57	3203.80	80.34						]]

[[

]]

Figure 5-1 Differences in MFLPD versus Core Power/Flow Ratio

[[

]]

Figure 5-2 Differences in MAPRAT versus Core Power/Flow Ratio

[[

]]

Figure 5-3 Differences in MFLCPR versus Core Power/Flow Ratio

Non-proprietary version

Figure 5-4 Slides from FLN-2002-015

GNF

Global Nuclear Fuel

A Joint Venture of GE, Toshiba, & Hitachi

Methods Technology Update

August 2002

Selected validation database

- ***PANAC10 compared with PANAC10/3DM evaluated thermal limit values***
  - *8 plants for 9 cycles containing GE13 and GE14 lead fuel for a total of 468 points.*
- ***PANAC11 compared with PANAC11/3DM evaluated thermal limit values***
  - *5 plants for 8 cycles containing GE12 and GE14 lead fuel for a total of 349 points.*

GNF Proprietary Information

[[

]]

[[

]]

References:

5-1 MFN 05-005, Letter from George Stramback (GE) to NRC, March 25, 2005, *Methods Interim Process (TAC No. MC5780)*

5-2 Letter from G.A. Watford (GE) to Alan Wang (NRC), FLN-2002-015, "NRC Technology Update - Proprietary Slides - July 31 - August 1, 2002", October 21, 2002.

NRC RAI 25

Core Follow Data: The objective of this review is to determine the accuracy of TGBLA and PANAC for the current operating strategies. The staff understands that GNF-A receives operating data from plants and performs offline PANAC calculations to monitor the plants' performance (i.e., eigenvalue tracking).

25-1 Select plants with challenging core designs (e.g., uprated plants and high-density plants with extended cycles) to benchmark the TGBLA and PANAC codes. The data from the plants should be statistically significant to current BWR operating strategies and fuel designs (GE14). The core tracking cycle exposure should extend to the number of cycles a fuel bundle may remain loaded in a core.

25-2 Provide plant-specific information for each set of core follow data (the plant type, whether the power level has been uprated, power density, operating domain, fuel type, cycle length, etc.). For each TIP reading, give the cycle state point, the operating power/flow state point, and the corresponding calculated thermal margin available. Evaluate the plant-specific data, including whether the core follow data indicates that the code is less accurate for higher in-channel void conditions. Explain any trends in the data in terms of operation at higher operating domain, cycle length, uprate and high high-density plants. Demonstrate that the current uncertainties and biases used in the NRC-approved analytical method (e.g. bundle power, σ P4B , power allocation factor, σ PALj, and pin power peaking etc) remain valid and applicable.

Proposed GE Response

Response 25-1:

Five BWRs have been selected for this study (Plants A-E), and they will be referred to as the **Reference BWRs, or Reference Plants**. Nine operating cycles have been selected for this study (two cycles for Plants A, B, C and E; one cycle for Plant D), and these cycles will be referred to as the **studied cycles**, or **cycles studied**. Table 25-1 provides the key performance characteristics of each of these Reference BWRs.

These reference plants have been selected because they operate at high power density, and cover a large range of plant sizes. All but Plant C, which operates on annual cycles, are operating on nominal two-year cycles. While the power density of Plant C is not as high as that of the other reference plants, it operates at very high bundle powers because of its small core size. The high bundle powers in this plant result in high bundle (or channel) exit void fractions, which are of interest for this study. The predominant fuel type in all of these plants is high (~4.0 w/o) enriched 10x10 fuel (GE14).

Two cycles of operation have been analyzed for all plants but Plant D. Only the current operating cycle is used for Plant D, since it is operating at its licensed power uprate of 120% in

the current cycle. Therefore, nine operating cycles are included in this study, which provides a statistically significant dataset for current operation at high power density in high-energy cycles.

RAI 25-1 requested that the core tracking cycle exposure extend to the number of cycles a fuel bundle may remain in the core. For two-year high-energy cycles, bundles typically remain in the core for two or three cycles. While a maximum of two cycles have been specifically analyzed in this study, the core tracking has been done for all previous cycles with the same nuclear methods (TGBLA06/PANAC11). Thus, the historical characteristics (e.g., nodal exposures and void histories) for all the fuel bundles that resided in the core in previous cycles are carried into the cycles being studied. The cycles being studied include fuel bundles that cover the entire range of exposures from fresh to highly exposed, and since all fuel characteristics are based on the nuclear methods being evaluated, the cycles being studied provide an appropriate representation of fuel at all exposures. The intent of the RAI request stated above is satisfied since all fuel in the core has been tracked using the methods being evaluated, and the fuel bundles resident in the core cover the full range of exposures in the cycles included in the study.

Response 25-2:

Introduction

This response will include a description of the key parameters for each cycle studied, followed by detailed data obtained from core tracking and TIP responses, and finally an analysis of this data.

Before presenting the detailed data, a brief overview of the cycles studied is provided. For Plant A, two cycles are studied, Cycles 18 and 19. Cycle 18 is of particular interest because it was uprated from 1658 MWT (104% OLTP) to 1912 MWt (120% OLTP) during this cycle. The early portion of the cycle was operated up to 104%, and then the power was increased to ~112% for the remainder of the cycle. Comparing the results of the core tracking before and after the power increase will provide insight into whether the fidelity of the core methods changes due to the increased power density and voiding in the core.

Plant B is a high power density BWR/6, but has a modest power uprate of 105%. Plant E is also a BWR/6, but it has been uprated to 120%, and has the highest power density of all the reference plants. Two cycles are studied for each of these BWR/6 plants, which coincidentally are Cycles 9 and 10 for both.

As mentioned earlier, Plant C is unique because of its small core size, which results in high bundle powers. These high bundle powers provide the opportunity to evaluate the nuclear methods for limiting high power bundles. Cycles 30 and 31 are studied for Plant C.

Plant D is a BWR/4 that began operating at its full licensed uprate power of 120% in Cycle 15. Cycle 15, the current operating cycle, is studied for this reference plant because of its high power density.

The core loading for each of the studied cycles is provided in the next section. The core loading data shows the steady progression to high-enriched GE14 fuel. It is also interesting to note that for the high-energy two-year cycles (plants A, B, D and E), the reload batch size is also increasing in most cases, with a maximum batch fraction of 50% for Plant E in Cycle 10. At the other extreme, for the annual cycles in Plant C, the reload batch size of 16.7% remains constant, and at the low end of the BWR experience range. The increase in cycle energy for this plant is achieved with increased enrichment, rather than with a combination of increased reload batch size and enrichment.

The following sections provide details of the cycles studied for each reference plant.

Key Core Parameters for the Reference Plants for Each Cycle Studied

This section summarizes the licensed operating domain, the nominal cycle length used to design the cycle, and the core loading for each of the nine cycles studied.

Plant A – Cycle 18

Licensed Thermal Power: 1912 MWt (120% of OLTP)
Flow Range at Licensed Power: 48.5 to 49.0 Mlbm/hr (99 – 100% of Rated Flow)
Nominal Cycle Length: 2 years
Core Loading:

Cycle Loaded	No. of Bundles	Fuel Type	Avg. Enrichment of Bundles Loaded
18	136	GE14 (10x10)	4.02
17	128	GE12 (10x10)	3.71
16	104	GE10 (8x8)	3.41

Plant A – Cycle 19

Licensed Thermal Power: 1912 MWt (120% of OLTP)
Flow Range at Licensed Power: 48.5 to 49.0 Mlbm/hr (99 –100% of Rated Flow)
Nominal Cycle Length: 2 years
Core Loading:

Cycle Loaded	No. of Bundles	Fuel Type	Avg. Enrichment of Bundles Loaded
19	152	GE14 (10x10)	4.11
18	136	GE14 (10x10)	4.02
17	80	GE12 (10X10)	3.71

Plant B – Cycle 9

Licensed Thermal Power: 3758 MWt (105% of OLTP)
Flow Range at Licensed Power: 84.2 to 109.2 Mlbm/hr (81-105% of Rated Flow)
Nominal Cycle Length: 2 years
Core Loading:

Cycle Loaded	No. of Bundles	Fuel Type	Avg. Enrichment of Bundles Loaded
9	304	GE14 (10x10)	4.16
8	278	GE12 (10x10)	3.99
7	166	GE12 (10x10)	3.69

Plant B – Cycle 10

Licensed Thermal Power: 3758 MWt (105% of OLTP)
Flow Range at Licensed Power: 84.2 to 109.2 Mlbm/hr (81-105% of Rated Flow)
Nominal Cycle Length: 2 years
Core Loading:

Cycle Loaded	No. of Bundles	Fuel Type	Avg. Enrichment of Bundles Loaded
10	280	GE14 (10x10)	4.13
9	304	GE14 (10x10)	4.16
8	164	GE12 (10x10)	3.99

Plant C – Cycle 30

Licensed Thermal Power: 1096.9 MWt (110% of OLTP)
Flow Range at Licensed Power: 25.84 to 33.0 Mlbm/hr (87 –111% of Rated Flow)
Nominal Cycle Length: 1 year
Core Loading:

Cycle Loaded	No. of Bundles	Fuel Type	Avg. Enrichment of Bundles Loaded
30	40	GE14 (10x10)	4.19
29	40	GE14 (10x10)	4.05
28	40	GE14 (10x10)	3.91
27	36 4	GE14 (10x10) GE11(9x9)	3.86
26	8 32	GE14 (10x10) GE11(9x9)	3.71
25	8	GE11(9x9)	3.60
24	17	GE11(9x9)	3.80
22	15	GE11(9x9)	3.60

Plant C – Cycle 31

Licensed Thermal Power: 1096.9 MWt (110% of OLTP)
Flow Range at Licensed Power: 25.84 to 33.0 Mlbm/hr (87 –111% of Rated Flow)
Nominal Cycle Length: 1 year
Core Loading:

Cycle Loaded	No. of Bundles	Fuel Type	Avg. Enrichment of Bundles Loaded
31	40	GE14 (10x10)	4.19
30	40	GE14 (10x10)	4.19
29	40	GE14 (10x10)	4.05
28	40	GE14 (10x10)	3.91
27	36 4	GE14 (10x10) GE11 (9x9)	3.86
26	8 28	GE14 (10x10) GE11 (9x9)	3.69
25	4	GE11(9x9)	3.80

Plant D – Cycle 15

Licensed Thermal Power: 2923 MWt (120% of OLTP)
Flow Range at Licensed Power: 76.2 to 80.5 Mlbm/hr (99 –104.5% of Rated Flow)
Nominal Cycle Length: 2 years
Core Loading:

Cycle Loaded	No. of Bundles	Fuel Type	Avg. Enrichment of Bundles Loaded
15	246	GE14 (10x10)	4.21
14	246	GE14 (10x10)	4.23
13	68	GE13 (9x9)	4.04

Plant E – Cycle 9

Licensed Thermal Power: 3473 MWt (120% of OLTP)
Flow Range at Licensed Power: 83.7 to 88.7 Mlbm/hr (99 –105% of Rated Flow)
Nominal Cycle Length: 2 years
Core Loading:

Cycle Loaded	No. of Bundles	Fuel Type	Avg. Enrichment of Bundles Loaded
9	268	GE14 (10x10)	3.89
8	188	GE14 (10x10)	3.53
7	168	GE10 (8x8)	3.53

Plant E – Cycle 10

Licensed Thermal Power: 3473 MWt (120% of OLTP)
Flow Range at Licensed Power: 83.7 to 88.7 Mlbm/hr (99 –105% of Rated Flow)
Nominal Cycle Length: 2 years
Core Loading:

Cycle Loaded	No. of Bundles	Fuel Type	Avg. Enrichment of Bundles Loaded
10	312	GE14 (10x10)	4.21
9	268	GE14 (10x10)	3.89
8	44	GE14 (10x10)	3.54

Core Tracking Data for Each of the Cycles Studied

The core tracking data is provided in tabular form in this section. For each of the cycles studied, the Core Power, Core Flow, Power Density, Core Average Exit Void Fraction, Maximum Channel Exit Void Fraction, Thermal Margins, and Hot Critical Eigenvalue will be provided as a function of cycle exposure. These data are taken directly from the exposure accounting analyses, and are based solely on calculations performed by the nuclear methods. There is no adaption to the process computer data included in these results. These results are provided in Tables 25-2 through 25-10.

The thermal margins are presented for each of the three related Tech Spec limits: Critical Power, Linear Heat Generation Rate and ECCS/LOCA. These limits are referred to as the MCPR, LHGR, and MAPLHGR limits, respectively. The core tracking data provides the ratio of the most limiting value of MCPR, LHGR, and MAPLHGR in the core to its respective limit. These ratios are identified as MFLCPR, MFLPD, and MAPRAT and are checked for compliance to Tech Specs by the core monitoring system. Thus, a statepoint with a MFLPD of 0.9 indicates that the highest LHGR in the core is 10% below the LHGR limit at this statepoint. Tables 25-2 through 25-10 shows that thermal margin values greater than 1.0 are infrequently obtained for MFLPD and MAPRAT. This is not unexpected for core states that are close to the thermal limits, since there is not perfect agreement between the nuclear methods and the plant monitoring measurements as formalized in the response to RAI 5-5. A MFLPD or MAPRAT value greater than 1.0 in these tables indicates that the nuclear methods over-predict the limiting nodal power at the given statepoint.

Cold critical eigenvalue data for each of the cycles studied is provided in Table 25-11. Cold critical data is provided for each point in the cycle where a cold critical test was performed. Table 25-11 shows the cycle exposure at which the test was performed, the measured cold critical eigenvalue, and the design basis eigenvalue which was selected for design purposes prior to operation. The design basis eigenvalues are selected by the responsible design engineer and are based on the prior history of the particular plant and known trends of the nuclear methods used for design. The measured cold critical eigenvalues are obtained by running the 3D Simulator at the same exposure and with the critical rod patterns used in the test. The eigenvalue calculated by the simulator is then corrected for the positive period measured during the test. The data in Table 25-11 include both distributed control rod patterns (as would occur during normal startup or shutdown) and local criticals where control rod(s) are withdrawn in a particular core location. Note that the design basis cold eigenvalue is not provided for Plant B, Cycle 9, and Plant E, Cycle 9. The reason for this exception is that when these cycles were being designed, PANAC10 was used, but the analysis of the test was performed with PANAC11. Therefore, the actual design basis eigenvalue was based on the earlier version of the 3D Simulator, and it would not be valid to compare it to the PANAC11-based measured eigenvalue.

TIP Data Summary for the Cycles Studied

Summary core-wide statistics for the TIP data taken during the cycles studied is provided in Table 25-12. (TIP analyses for local four-bundle cells are provided in the responses to RAIs 27 and 29.) This table provides the cycle exposure at which the TIP data was taken, the core power and flow, the RMS differences between the TIP data and the power distribution calculated by the 3D Simulator, the core average and maximum channel exit void fractions, and the thermal margins calculated by the 3D Simulator at each of the TIP statepoints. The RMS differences are calculated for the Bundle (Radial), Axial and Nodal quantities at each statepoint. Definitions of these quantities, and the equations used to calculate them are provided in the response to RAI 21 2.

TIP data for Plant D, Cycle 15 are not included in Table 25-12 because they are not yet available for processing for this cycle, which is currently in operation. However, Table 25-12 contains a significant amount of data at high power density from Cycles 9 and 10 of Plant E, which were licensed to 120% power.

Evaluation of the Core Tracking Data and TIP Comparisons

The purpose of this section is to analyze the plant-specific data provided above to determine whether the nuclear methods are less accurate for higher in-channel void conditions and to explain any trends observed which may result from operation higher in the operating domain at higher power/flow ratios (e.g. from power uprate and in high power density plants). In addition, to analyze any trends that may be attributed to longer cycle lengths and higher cycle energies, both of which increase the cycle exposure.

The results of these analyses will be discussed relative to the current uncertainties and biases used in the NRC-approved analytical methods. The hot and cold critical eigenvalues and TIP data comparisons will yield biases and uncertainties that can be compared to the current uncertainties. [[

]] If the TIP response continues to confirm methods adequacy, it is statistically improbable that the [[ ]] would need to be revised. RAI 28 further addresses the relationship between the gamma scans and the SLMCPR uncertainties. RAI 30 addresses pin power peaking via lattice benchmarking, and requires development of uncertainties for both pin power peaking and bundle power.

To gain an appreciation of where the Reference Plants typically operate on the core Power/Flow Map, the Power/Flow Map is provided for each plant and the operating statepoints throughout each cycle are plotted on this map. Figures 25-1 through 25-9 provide these Power/Flow Maps. From these figures, it may be seen that the plants operate over a fairly wide flow range at, or near, licensed power. Plant A operates near licensed power between 90-100% flow, Plant B from 85-

105% flow, Plant C from 90-111% flow, Plant D from 99-105% flow, and Plant E from 95-100% flow.

There is a scattering of data points on these Power/Flow maps at low power/low flow conditions. Plant A, Cycle 18, has the largest number of these data points, which makes it the ideal case to study the characteristics of these off-rated conditions. Of most interest for this study is the impact of power/flow state on exit void fractions. Figure 25-10 has been constructed to answer this question.

Figure 25-10 shows the core average exit and maximum channel exit void fractions for each data point on the Power/Flow map for this cycle (Figure 25-1). The data have been divided into two regions on the Power/Flow map, those at core flows <87%, and those at core flows >87%. Consideration of Figure 25-1 shows that for the Plant A, Cycle 18 data, 87% flow is a convenient dividing line between the high power/high flow statepoints above 100% OLTP, and those off-rated points which are not only at lower power, but are at lower flows. Essentially the same result would have been obtained by dividing the data points into two sets above and below 100% OLTP, but a few low power points at high flow (with low void fractions) would have been included in the low power off-rated data set.

Figure 25-10 shows that while some of the low power/low flow state points result in core average and maximum channel exit void fractions that are close to those at high power, their exit void fractions do not exceed those for the high power statepoints. Also, the majority of the high exit void fraction data are from the high power conditions for which the flow is near the MELLLA Limit. While it may be possible for an off-rated point very close the MELLLA limit to have higher exit void fractions, the data shows that this is not a likely operating state, and because the preponderance of the data for high void operation is at high power, the amount of exposure accumulation in such an off-rated condition would be negligible.

The data in Figure 25-10 show that the off-rated conditions are not expected to result in exit void fractions greater than those produced at high power and flow. Secondly, because the accumulation of exposure in the core is predominantly the result of high power operation, the impact of off-rated conditions on exposure accumulation in the fuel is negligible. Therefore, it is concluded that the off-rated conditions at low core powers need not be considered to study of the effect of high voiding on the nuclear methods.

However, operation at the low end of the licensed flow range near rated power does occur frequently, and does result in the highest voiding conditions in the core. The impact on methods fidelity of these statepoints is considered in both RAIs 25 and 26.

Analysis of Hot Critical Eigenvalues

In plant tracking calculations, the 3D Simulator (using cross sections generated from the lattice physics model, thermal-hydraulic models, and all other model assumptions) is used to simulate the behavior of a plant during operation. The reactor power, total core flow, pressure, inlet conditions, and reactivity control inventory as a function of cycle exposure are all involved in the prediction of the critical state of the core. The actual operating reactor is critical; hence, the calculated k_{eff} is compared to 1.0. Accurate and technically well-founded simulators calculate a k_{eff} that is predictable and should not vary appreciably from cycle-to-cycle for any particular plant. Any trends in fuel exposure should be small and reproducible. Consistency of k_{eff} bias ensures that accurate cycle length estimates are obtained in future core designs.

Figure 25-11 plots the hot critical eigenvalues for all the studied cycles. The trendline for all the eigenvalue data in Figure 25-11 "Linear (Trendline for all Data)," has been added to show the trend of the data with cycle exposure. This trend is very typical for the BWR hot critical eigenvalues predicted by GE's nuclear methods. The data which are widely dispersed from the trendline, particularly for Plant A, reflects substantial deviations from steady conditions and does not affect the ability of the plant to correctly determine end of full power capability. The RMS difference between the eigenvalue data for the studied cycles and the trendline is approximately [[ ]], which is substantially the same as reported in NEDC-30130P-A (Steady-state Nuclear Methods, 1985.)

By comparing the individual cycle data to the trendline, [[ ]] This data will be discussed in more detail below, in the section that compares the hot critical eigenvalues of Plant E for Cycles 8 and 9.

Also, Plant C is somewhat different in that its eigenvalue decreases at a steeper slope than for the other plants. This plant is unique in that it is the smallest BWR in the GE fleet, and is the only Reference Plant that operates on an annual cycle. The eigenvalues for this plant are very repeatable from cycle-to-cycle, and therefore lead to reliable predictions for design purposes.

The impact of increases in power density, Power/Flow Ratio, and void fractions will be examined by analyzing the behavior of the hot critical eigenvalues before and after significant power increases at two different plants. By using data from the same plant, it is possible to get a more direct comparison of the impact of a power increase than by trying to compare the eigenvalues from two different plants that operate at different power densities. Plants A and E will each be analyzed since they have had significant power increases since the introduction of two-year cycles and 10x10 fuel.

Hot Critical Eigenvalues for Plant A, Cycle 18

To study the impact of power density, Power/Flow Ratio and exit void fraction on hot critical eigenvalues, Plant A, Cycle 18 has been selected because it operated at 104% power during the first 4 GWD/ST of the cycle, and then increased its power to 112% for the remainder of the cycle (see Table 25-2). Figure 25-12 shows how core power and flow varied during this cycle. Note that when the power increased to 112%, the core flow remained at about the same value of 95%. Therefore, there should have been essentially a step change in core Power/Flow Ratio. The values of core Power/Flow Ratio, which is simply the ratio of the total core power to the total core flow, are shown in Figure 25-13. This figure shows that the core Power/Flow data are roughly divided at a value of 37, which is expressed in units of MWt/Mlbm/hr, before and after the power increase around 4 GWD/ST. Since exit void fractions are directly related to the core Power/Flow Ratio, exit void fractions were plotted vs. core Power/Flow Ratio in Figure 25-14. This figure shows that for both the core average and maximum channel exit void fractions, a core Power/Flow value of 37 is a reasonable boundary between the exit void fraction data before and after the power increase. Below 37, the exit void fractions increase appreciably with Power/Flow Ratio, but above 37, they tend to level off.

Finally, Figure 25-15 was constructed to examine the behavior of the hot critical eigenvalue as a function of core Power/Flow Ratio (and indirectly as a function of power density and exit void fraction) for Plant A, Cycle 18. This figure divides the eigenvalue data between those values obtained from operating states with a core Power/Flow Ratio below 37 MWt/Mlbm/hr, and those for which the core Power/Flow Ratio is above 37. The trend of the eigenvalues from one core Power/Flow region to the other shows no discontinuity between the two data sets, and indicates that there is no discernible impact of the higher core Power/Flow Ratios (or the consequential higher void fractions and power densities) on the eigenvalue trend for this cycle.

Hot Critical Eigenvalues for Plant E, Cycles 8 and 9

Another comparison of hot eigenvalues before and after a significant power uprate is made by comparing Cycles 8 and 9 for Plant E. Cycle 8 was the last cycle of operation prior to the 120% power uprate in Cycle 9. The Cycle 8 exposure accounting data are provided in Table 25-13 (at the end of this section), since this was not one of the high power density cycles included in Tables 25-2 thru 25-10.

Figure 25-16 compares the power density and core Power/Flow Ratio for Cycles 8 and 9. The power density increased by ~10%, from 52.5 kW/l in Cycle 8 to an average of about 58% in Cycle 9. The core Power/Flow Ratio also increased from ~37.5 to 41-42 MWt/Mlbm/hr. Also, the cycle exposure (and cycle energy) increased significantly from 11.5 to 16.0 GWD/ST. This increase in cycle energy was achieved by increasing the reload batch size from 188 to 268 GE14 bundles, and by increasing the average enrichment of the reload bundles from 3.53 to 3.89w/o.

Figure 25-17 compares the hot critical eigenvalues for Cycles 8, 9 and 10. This figure shows very little change in the eigenvalue from Cycle 8 to Cycle 9, in spite of the significant changes in cycle energy, power density, reload batch size, and reload enrichment.

As mentioned earlier, [[
]] as shown in both Figures 25-11 and 25-17. From the Power/Flow maps shown in Figures 25-8 and 25-9, it is clear that both Cycles 9 and 10 for Plant E operated at the essentially the same power (~115%) and over the same flow range at this power level. Thus, there is no difference in power density and Power/Flow Ratio, and no significant change in exit void fractions (see Tables 25-9 and 25-10) for these two cycles. [[

]] This was the first time such a large batch size had been used, and it resulted in a loading pattern that placed high reactivity fuel on the core periphery. This loading pattern resulted in higher fast neutron leakage from the core, which could be contributing to the hot eigenvalue differences. The TIP RMS differences presented in Table 25-12 for Cycle 10 indicate that the core power distribution is being tracked reliably for this cycle. From Table 25-11, the two cold eigenvalue data points show excellent agreement between the measured and design basis cold eigenvalues for Cycle 10, [[
]] Because fast neutron leakage in a cold, unvoided core is much less than at the hot condition, this also may be an indication that fast neutron leakage may be underestimated at high power by the nuclear methods for this unique core loading. This cycle is being closely monitored and will be studied further to understand its hot eigenvalue trend.

Conclusions

The hot critical eigenvalues for the studied cycles, [[
]] show the same general trends as seen in previous BWR operating cycles. Examination of the impact of power density, Power/Flow Ratio, and void fractions on the hot eigenvalues showed no apparent sensitivity to these parameters for the two plants studied (A and E). [[

]] While the noted differences exist for the hot critical eigenvalues in this latest cycle, the cold critical eigenvalues and 3D power distribution comparisons to the TIP measurements are in good agreement.

Finally, it is noted that the significant increase in cycle energy for Plant E when transitioning from Cycle 8 to Cycle 9 did not result in a change in the hot critical eigenvalue trend with cycle exposure.

Analysis of Cold Critical Eigenvalues

BWRs are designed so that they can be shut down in the cold condition (68°F) with the single strongest control blade completely withdrawn. In order to qualify the 3D Simulator to accurately predict the cold shutdown margin, cold critical startup configurations are analyzed. In all cases,

enough control blades were withdrawn at a given water temperature for the reactor to be critical or on a large positive period. Accurate and technically well-founded simulators calculate a k_{eff} that is predictable and should not vary appreciably from cycle-to-cycle for any particular plant. Any trends in fuel exposure should be small and reproducible. Consistency of k_{eff} bias ensures that accurate shutdown margin estimates will be obtained in future core designs.

Figure 25-18 shows cold critical eigenvalue data for all of the studied cycles. These are the same measured eigenvalues presented in Table 25-11. For convenience, the linear trend line for all this data is plotted, "Linear (Trend Line using all Data)," showing the typical reduction in eigenvalue as the core depletes. This trend is very consistent with the eigenvalue trend used in the development of the nuclear design basis in the GNF reload design process. Although the startup sequence, configurations and conditions may vary considerably between plants, the data do not show greater than expected dispersion of the critical eigenvalues. These data also contain some local critical configurations. The RMS difference between the predicted Nuclear Design Basis eigenvalue (also provided in Table 25-11) and the actual measured critical eigenvalue is [[ ]] for the cycles studied, which is substantially the same as the [[ ]] reported in NEDC-30130P-A (Steady-State Nuclear Methods, 1985).

To determine if there was any sensitivity to power density, the RMS difference between predicted and measured cold critical eigenvalues was calculated for the three Reference plants with the highest power density. The RMS difference was [[ ]] for these plants; namely, Plants B, D and E. Therefore, it is concluded that the cold critical eigenvalues show no discernible trend with power density. This behavior implies that there is also no trend with historical void fraction.

Next, the RMS difference between predicted and measured cold critical eigenvalues was calculated for Plant C, the only plant operating on an annual cycle. The RMS for both cycles studied for Plant C was [[ ]]. This value is somewhat better than the [[ ]] obtained for all the studied cycles, but the difference between these two values does not indicate a trend in accuracy with cycle length.

In conclusion, the analysis of the cold critical eigenvalues for all of the cycles studied shows that they are well predicted by the nuclear methods, and that there are no discernible trends in accuracy of this key parameter with power density, void fraction, or cycle length.

Uncertainties and biases in NRC-approved methods

In addition to the prior examination of data from operating plant experience, the TIP data from the Reference Plants may be used to determine whether the uncertainties and biases in NRC approved analytical methods remain valid. This evaluation uses the TIP RMS data tabulated in Table 25-12. This data represents the RMS differences for all operable TIP strings at each reactor statepoint at which the TIP data were obtained. RAIs 27 and 29 deal directly with a more

detailed comparison of the TIP and 3D Simulator results for hot channels and limiting four-bundle cells.

To determine if there are any observable trends in RMS differences as the power density is increased and the operating domain is expanded, it is necessary to identify a meaningful correlating parameter, such as power density, core Power/Flow Ratio, or exit void fractions. Power density alone does not directly include the impact of different core flows at the same power density, and as such is not an appropriate correlating parameter. The core average exit void fraction, or the maximum channel exit void fraction would appear to be good correlating parameters, but a review of Table 25-12 shows that they do not span a very large range for the studied plants, even though there is a fairly wide range of power densities and operating flow ranges. Therefore, the core Power/Flow Ratio has been selected as the correlating parameter since there is a direct relationship between this parameter and the amount of voiding in the core. It can easily be shown to be relevant to EPU/MELLLA+ conditions, and it covers a sufficiently broad range in the cycles studied to perform trending analyses.

All of the Reference Plants have Gamma TIPs except Plant E, which has Thermal Neutron TIPS. Because of the differences in the sensitivity of these TIP systems, the RMS differences also vary. Figure 25-19 plots the core-wide Bundle (Radial), Axial and Nodal RMS differences for each of the TIP statepoints for the Gamma TIP plants. Figure 25-20 provides the same data for the Thermal TIP plant.

[[

]]

Extrapolating the trend lines for the Gamma TIP plants to 50 MWt/Mlbm/hr, the Nodal and Axial RMS values would be on the order of 6%, while the Bundle RMS would be less than 2%. A Power/Flow Ratio of 50 MWt/Mlbm/hr is expected to bound the Power/Flow Ratio for EPU/MELLLA+ operation. For example, for Plant E, which is a BWR/6, and has the highest power density of the five Reference Plants, the Power/Flow Ratio at 120% power and 85% flow is 48.4 MWt/Mlbm/hr. The maximum Power/Flow Ratio for EPU/MELLLA+ occurs at 120% power and 85% flow.

The small number of data points in Figure 25-19 for the Thermal Neutron TIP plants is insufficient to draw any definite conclusions. [[

]]

It is interesting to note that for Plant E, Cycle10, the maximum RMS values recorded in Table 25-12 throughout the entire cycle were [[ ]] for the Bundle, Axial and Nodal RMS, respectively. This indicates that the power shapes generated by the 3D Simulator are in good agreement with the TIP measurements, even though this cycle has hot eigenvalues that were higher than expected early in the cycle.

The TIP comparison results are within the results previously provided to the NRC. Furthermore, the new results compare favorably with the uncertainties compiled earlier for TGBLA06/ PANAC11. The quantity to consider is the RMS difference between the calculated and measured Bundle TIP response. This RMS difference is used in part to determine the bundle power uncertainty in the Process Computer and is an input to the SLMCPR evaluation. The results are summarized below for NEDE-32694 (Power Distribution Uncertainties for Safety Limit MCPR Evaluations, 1999), which is the basis for the SLMCPR evaluations, a set of comparisons documented in 1999 (NEDE-32773-R1) for the TGBLA06/ PANAC11 model, and the results quoted for this analysis taken from the eight cycles studied. The results are shown in Table 25-14.

The data in Figures 25-19 and 25-20 demonstrate that not only is the Bundle RMS difference calculated from the eight studied cycles applicable to the range of operating experience for the high power density cycles studied in this response, but that this population of data is consistent with previous experience, as illustrated in Table 25-14.

In conclusion, the global comparison of TIP RMS differences for the eight studied cycles shows good agreement between the TIP measurements and the 3D Simulator. [[

]]

Table 25-1. Key Core Parameters for Reference Plants

Plant	GE BWR Type	Number of Bundles	Original Licensed Thermal Power (OLTP) MWt	Rated Flow (Flow at OLTP) Mlbm/hr	Licensed Power Uprate (PU) % OLTP	Licensed Core Flow Range at PU % Rated Flow	Power Density at Licensed PU kW/l
A	BWR/4	368	1593	49.0	120	99-100	58.7
B	BWR/6	748	3579	104.0	105	81-105	56.8
C	BWR/4	240	997.2	29.7	110	87-111	51.7
D	BWR/4	560	2436	77.0	120	99-105	59.0
E	BWR/6	624	2894	84.5	120	99-107	62.9

Non-proprietary version

Table 25-2: Exposure Accounting Data for Plant A, Cycle 18

Cycle Expo. GWD/ST	Core Power % OLTP	Core Flow % Rated	Power Density kW/l	Avg. Core Exit Void Fract.	Max. Chan. Exit Void Fract.	MFLCPR	MFLPD	MAPRAT	Hot Critical Eigen-value
0.02	34.1	55.3	16.7	0.54	0.66	[[			
0.03	60.8	55.7	29.7	0.70	0.77				
0.17	77.9	79.2	38.1	0.70	0.77				
0.21	82.7	63.5	40.4	0.75	0.83				
0.34	104.2	98.1	51.0	0.73	0.81				
0.37	48.2	57.8	23.6	0.63	0.71				
0.38	83.7	65.6	40.9	0.75	0.82				
0.41	104.1	97.0	50.9	0.74	0.81				
0.72	104.0	96.9	50.9	0.73	0.81				
0.75	55.2	57.4	27.0	0.67	0.74				
0.78	104.1	94.9	50.9	0.74	0.82				
1.05	104.0	95.2	50.8	0.74	0.82				
1.16	103.9	93.2	50.8	0.74	0.82				
1.21	103.9	93.4	50.8	0.74	0.82				
1.25	89.0	72.2	43.5	0.75	0.83				
1.26	50.5	56.2	24.7	0.65	0.73				
1.28	103.7	97.8	50.7	0.73	0.81				
1.44	103.9	96.1	50.8	0.74	0.81				
1.61	104.1	94.6	50.9	0.74	0.82				
1.64	86.9	71.2	42.5	0.74	0.84				
1.66	103.9	97.8	50.8	0.73	0.83				
1.91	104.0	95.2	50.9	0.73	0.84				
2.14	104.1	94.5	50.9	0.74	0.84				
2.34	104.0	93.1	50.9	0.74	0.84				
2.66	104.1	93.6	50.9	0.74	0.84				
2.73	104.0	92.5	50.9	0.74	0.84				
3.04	104.0	93.3	50.9	0.74	0.84				
3.06	47.1	76.6	23.1	0.56	0.71				
3.07	50.0	68.4	24.5	0.59	0.74				
3.09	99.2	85.6	48.5	0.74	0.85				
3.21	103.8	96.2	50.8	0.73	0.84				
3.37	104.1	95.9	50.9	0.73	0.84				
3.41	103.8	95.6	50.8	0.73	0.84				
3.43	72.6	73.8	35.5	0.69	0.79				
3.45	94.2	75.1	46.1	0.75	0.86				
3.47	100.4	85.8	49.1	0.74	0.85				
3.51	104.0	92.4	50.8	0.74	0.85				

Non-proprietary version

Table 25-2: Exposure Accounting Data for Plant A, Cycle 18

Cycle Expo. GWD/ST	Core Power % OLTP	Core Flow % Rated	Power Density kW/l	Avg. Core Exit Void Fract.	Max. Chan. Exit Void Fract.	MFLCPR	MFLPD	MAPRAT	Hot Critical Eigen-value
3.55	98.1	81.3	48.0	0.75	0.86				
3.57	104.0	91.8	50.8	0.74	0.85				
3.60	107.8	94.4	52.7	0.75	0.85				
3.69	110.5	95.6	54.0	0.75	0.86				
3.96	112.3	96.0	54.9	0.75	0.86				
4.50	111.7	94.5	54.6	0.75	0.86				
4.63	112.4	95.6	55.0	0.75	0.86				
4.64	59.9	61.3	29.3	0.67	0.77				
4.67	112.1	97.9	54.8	0.75	0.86				
4.96	111.0	98.6	54.3	0.74	0.86				
5.25	111.1	96.6	54.3	0.74	0.86				
5.26	53.1	49.8	26.0	0.67	0.78				
5.28	94.0	72.8	46.0	0.76	0.85				
5.31	111.0	93.2	54.3	0.75	0.85				
5.57	111.0	95.4	54.3	0.75	0.84				
5.77	111.0	94.1	54.3	0.75	0.85				
5.94	111.1	93.1	54.3	0.75	0.85				
6.13	111.0	96.4	54.3	0.75	0.84				
6.15	89.1	80.6	43.6	0.72	0.84				
6.17	108.7	88.6	53.1	0.76	0.85				
6.37	112.2	95.1	54.9	0.75	0.85				
6.57	112.2	94.4	54.9	0.75	0.85				
6.91	112.2	96.6	54.9	0.75	0.85				
7.16	112.3	94.7	54.9	0.75	0.85				
7.18	112.3	94.6	54.9	0.75	0.86				
7.40	112.5	96.6	55.0	0.75	0.86				
7.62	112.3	94.9	54.9	0.75	0.86				
7.82	112.4	93.8	55.0	0.75	0.86				
7.85	112.4	96.6	55.0	0.75	0.86				
7.88	76.2	64.9	37.3	0.72	0.85				
7.90	111.0	90.1	54.3	0.75	0.87				
7.92	112.3	95.9	54.9	0.75	0.86				
8.14	112.2	94.2	54.9	0.75	0.86				
8.42	112.4	93.7	55.0	0.75	0.87				
8.64	112.1	96.2	54.8	0.74	0.86				
8.86	112.3	95.6	54.9	0.75	0.86				
9.10	112.4	94.6	55.0	0.75	0.87				
9.13	111.2	98.2	54.4	0.74	0.86				

Non-proprietary version

Table 25-2: Exposure Accounting Data for Plant A, Cycle 18

Cycle Expo. GWD/ST	Core Power % OLTP	Core Flow % Rated	Power Density kW/l	Avg. Core Exit Void Fract.	Max. Chan. Exit Void Fract.	MFLCPR	MFLPD	MAPRAT	Hot Critical Eigen-value
9.15	112.2	96.7	54.9	0.74	0.86				
9.42	112.3	95.3	54.9	0.75	0.87				
9.68	112.5	95.3	55.0	0.75	0.87				
9.69	47.3	60.4	23.1	0.57	0.77				
9.72	109.8	91.2	53.7	0.75	0.87				
9.74	112.2	95.2	54.9	0.75	0.87				
10.06	112.2	93.9	54.9	0.75	0.87				
10.09	109.2	94.6	53.4	0.74	0.86				
10.11	66.8	65.0	32.7	0.68	0.83				
10.13	78.8	89.9	38.5	0.66	0.82				
10.18	77.8	59.5	38.1	0.73	0.86				
10.20	80.4	71.1	39.3	0.72	0.85				
10.22	112.4	94.1	55.0	0.75	0.87				
10.35	112.3	97.3	54.9	0.74	0.86				
10.62	112.2	96.0	54.9	0.74	0.86				
10.79	112.2	94.1	54.9	0.75	0.86				
11.01	112.3	95.4	54.9	0.75	0.86				
11.03	67.4	68.5	33.0	0.67	0.80				
11.04	77.2	67.9	37.8	0.71	0.83				
11.07	109.7	89.9	53.7	0.75	0.87				
11.26	112.5	97.1	55.0	0.74	0.85				
11.49	112.2	94.0	54.9	0.75	0.86				
11.71	112.3	96.3	54.9	0.74	0.85				
11.90	112.4	94.1	55.0	0.75	0.86				
12.13	112.3	96.8	54.9	0.74	0.85				
12.35	112.3	93.7	54.9	0.75	0.85				
12.57	112.4	97.1	55.0	0.74	0.85				
12.69	112.4	96.0	55.0	0.74	0.85				
12.91	112.4	97.0	55.0	0.74	0.86				
13.23	112.5	96.0	55.0	0.74	0.86				
13.25	84.6	73.8	41.4	0.72	0.85				
13.28	112.5	94.5	55.0	0.74	0.87				
13.37	112.4	97.7	55.0	0.74	0.86				
13.58	112.5	95.7	55.0	0.74	0.86				
13.59	71.2	53.6	34.8	0.73	0.85				
13.62	104.5	99.2	51.1	0.72	0.85				
13.64	112.2	97.7	54.9	0.74	0.86				
13.89	112.3	93.4	54.9	0.74	0.87				

Non-proprietary version

Table 25-2: Exposure Accounting Data for Plant A, Cycle 18

Cycle Expo. GWD/ST	Core Power % OLTP	Core Flow % Rated	Power Density kW/l	Avg. Core Exit Void Fract.	Max. Chan. Exit Void Fract.	MFLCPR	MFLPD	MAPRAT	Hot Critical Eigen-value
13.98	112.3	96.8	54.9	0.74	0.86				
14.08	112.1	96.9	54.8	0.74	0.86				
14.16	112.4	98.1	55.0	0.73	0.86				
14.23	112.3	98.1	54.9	0.73	0.86				
14.30	112.4	98.7	55.0	0.73	0.86				
14.35	112.2	98.3	54.9	0.73	0.86				
14.45	112.3	98.3	54.9	0.73	0.86				]]

Non-proprietary version

Table 25-3: Exposure Accounting Data for Plant A, Cycle 19

Cycle Expo. GWD/ST	Core Power % OLTP	Core Flow % Rated	Power Density kW/l	Avg. Core Exit Void Fract.	Max. Chan. Exit Void Fract.	MFLCPR	MFLPD	MAPRAT	Hot Critical Eigen-value
0.02	62.6	65.2	30.6	0.68	0.75	[[			
0.04	109.0	88.8	53.3	0.76	0.83				
0.07	112.2	96.7	54.9	0.76	0.82				
0.19	112.3	96.5	54.9	0.76	0.82				
0.24	112.4	94.9	55.0	0.76	0.83				
0.51	112.4	96.3	55.0	0.76	0.83				
0.85	112.4	95.3	55.0	0.76	0.83				
1.10	112.4	93.3	55.0	0.76	0.83				
1.17	112.4	92.4	55.0	0.76	0.83				
1.47	112.4	94.6	55.0	0.76	0.84				
1.76	112.1	93.0	54.8	0.76	0.84				
2.06	112.4	94.8	55.0	0.76	0.84				
2.13	112.4	94.3	55.0	0.76	0.84				
2.38	112.3	93.9	54.9	0.76	0.84				
2.40	111.9	95.5	54.7	0.75	0.85				
2.43	112.3	97.4	54.9	0.75	0.85				
2.50	112.3	95.3	54.9	0.76	0.85				
2.72	112.3	94.8	54.9	0.76	0.85				
3.04	112.2	93.4	54.9	0.76	0.85				
3.06	112.2	93.2	54.9	0.76	0.85				
3.16	112.5	96.7	55.0	0.75	0.85				
3.38	112.4	96.4	55.0	0.75	0.85				
3.72	112.2	95.4	54.9	0.75	0.85				
4.04	112.5	94.1	55.0	0.76	0.86				
4.19	112.4	93.4	55.0	0.76	0.86				
4.36	112.3	92.9	54.9	0.76	0.86				
4.43	112.3	96.6	54.9	0.75	0.85				
4.51	112.5	97.8	55.0	0.75	0.84				
4.80	112.3	97.1	54.9	0.75	0.84				
4.87	31.9	52.2	15.6	0.53	0.66				
5.18	112.5	97.7	55.0	0.75	0.84				
5.41	112.4	98.1	55.0	0.75	0.84				
5.52	112.2	94.5	54.9	0.76	0.85				
5.79	112.2	96.6	54.9	0.75	0.84				
6.01	112.6	96.0	55.0	0.75	0.84				
6.26	112.3	94.3	54.9	0.76	0.85				
6.51	112.3	93.4	54.9	0.76	0.85				

Non-proprietary version

Table 25-3: Exposure Accounting Data for Plant A, Cycle 19

Cycle Expo. GWD/ST	Core Power % OLTP	Core Flow % Rated	Power Density kW/l	Avg. Core Exit Void Fract.	Max. Chan. Exit Void Fract.	MFLCPR	MFLPD	MAPRAT	Hot Critical Eigen-value
6.73	112.4	92.1	55.0	0.76	0.85				
6.95	112.4	95.4	55.0	0.75	0.85				
6.97	92.8	99.1	45.4	0.70	0.80				
6.99	112.4	94.0	55.0	0.76	0.86				
7.22	112.4	94.2	55.0	0.75	0.86				
7.39	112.5	93.9	55.0	0.76	0.86				
7.61	112.5	92.4	55.0	0.76	0.86				
7.95	112.4	96.0	55.0	0.75	0.85				
8.13	112.4	94.1	55.0	0.75	0.86				
8.17	112.4	93.8	55.0	0.76	0.86				
8.19	96.9	95.1	47.4	0.72	0.82				
8.21	64.2	53.9	31.4	0.70	0.81				
8.24	112.2	97.4	54.9	0.75	0.85				
8.26	112.3	97.1	54.9	0.75	0.85				
8.28	59.3	54.5	29.0	0.69	0.78				
8.30	111.8	91.9	54.7	0.76	0.86				
8.57	112.2	96.7	54.9	0.75	0.85				
8.84	112.1	96.7	54.8	0.75	0.85				
9.02	112.4	95.9	55.0	0.75	0.86				
9.14	112.4	95.6	55.0	0.75	0.86				]]

Non-proprietary version

Table 25-4: Exposure Accounting Data for Plant B, Cycle 9

Cycle Expo. GWD/ST	Core Power % OLTP	Core Flow % Rated	Power Density kW/l	Avg. Core Exit Void Fract.	Max. Chan. Exit Void Fract.	MFLCPR	MFLPD	MAPRAT	Hot Critical Eigen-value
0.26	105.1	100.0	56.8	0.74	0.83	[[			
0.39	104.8	99.0	56.7	0.74	0.83				
0.54	104.9	91.1	56.8	0.76	0.84				
0.79	104.9	90.8	56.8	0.76	0.84				
0.93	77.4	103.4	41.9	0.64	0.78				
1.16	104.9	96.4	56.8	0.74	0.83				
1.42	105.1	97.0	56.8	0.74	0.83				
1.61	104.9	94.4	56.7	0.75	0.84				
1.89	105.0	93.6	56.8	0.75	0.85				
2.20	104.9	90.4	56.8	0.76	0.85				
2.50	104.7	89.5	56.7	0.76	0.86				
2.80	105.1	88.5	56.8	0.76	0.86				
3.11	105.0	87.4	56.8	0.76	0.86				
3.41	104.7	84.8	56.7	0.77	0.87				
3.49	104.8	84.5	56.7	0.77	0.87				
3.69	105.0	86.1	56.8	0.76	0.87				
3.87	104.9	84.8	56.7	0.77	0.87				
4.12	104.9	85.2	56.7	0.77	0.87				
4.39	105.1	91.7	56.9	0.75	0.86				
4.67	105.0	90.4	56.8	0.75	0.86				
4.98	104.8	88.9	56.7	0.76	0.86				
5.22	104.9	88.8	56.7	0.76	0.86				
5.35	104.9	87.8	56.8	0.76	0.87				
5.47	89.3	91.4	48.3	0.71	0.81				
5.69	104.8	87.8	56.7	0.76	0.86				
5.92	105.0	87.9	56.8	0.76	0.86				
6.06	105.0	87.1	56.8	0.76	0.86				
6.23	104.7	96.9	56.6	0.74	0.85				
6.36	104.9	87.4	56.7	0.76	0.86				
6.63	104.9	87.2	56.8	0.76	0.87				
6.92	104.7	85.9	56.6	0.76	0.87				
7.20	104.8	97.5	56.7	0.74	0.86				
7.48	104.7	96.0	56.6	0.74	0.86				
7.76	105.0	95.1	56.8	0.74	0.86				
8.04	104.8	92.3	56.7	0.75	0.87				
8.31	105.1	89.9	56.9	0.75	0.87				
8.49	105.0	92.3	56.8	0.75	0.87				

Non-proprietary version

Table 25-4: Exposure Accounting Data for Plant B, Cycle 9

Cycle Expo. GWD/ST	Core Power % OLTP	Core Flow % Rated	Power Density kW/l	Avg. Core Exit Void Fract.	Max. Chan. Exit Void Fract.	MFLCPR	MFLPD	MAPRAT	Hot Critical Eigen-value
8.74	104.9	93.6	56.8	0.75	0.86				
8.97	104.8	92.4	56.7	0.75	0.87				
9.20	104.9	90.5	56.8	0.75	0.87				
9.33	104.9	95.8	56.8	0.74	0.86				
9.38	104.7	98.4	56.6	0.73	0.86				
9.58	105.0	100.6	56.8	0.73	0.85				
9.79	104.7	99.5	56.6	0.73	0.85				
10.06	104.9	100.7	56.7	0.73	0.85				
10.34	105.0	100.4	56.8	0.73	0.85				
10.56	105.2	100.0	56.9	0.73	0.85				
10.84	105.1	99.3	56.9	0.73	0.86				
11.12	105.0	99.3	56.8	0.73	0.85				
11.40	105.1	99.7	56.8	0.73	0.85				
11.70	105.1	100.0	56.8	0.73	0.85				
11.86	104.8	95.6	56.7	0.74	0.86				
12.00	101.2	103.4	54.7	0.71	0.85				
12.20	104.1	103.6	56.3	0.72	0.86				
12.37	103.2	103.9	55.8	0.71	0.85				
12.65	105.1	96.1	56.8	0.73	0.87				
12.93	105.0	100.0	56.8	0.73	0.86				
13.21	104.8	102.3	56.7	0.72	0.85				
13.26	104.5	103.5	56.5	0.72	0.85				
13.45	104.9	90.9	56.8	0.75	0.87				
13.71	105.1	94.5	56.8	0.74	0.86				
13.96	104.2	97.1	56.4	0.73	0.86				
14.24	104.7	97.9	56.6	0.73	0.86				
14.49	104.5	103.3	56.5	0.72	0.84				
14.76	104.9	103.0	56.8	0.72	0.85				
14.86	103.8	103.8	56.1	0.72	0.84				
15.03	104.5	103.9	56.5	0.71	0.85				
15.21	102.1	104.5	55.2	0.71	0.84				
15.34	101.1	105.0	54.7	0.70	0.83				
15.50	88.5	104.5	47.9	0.67	0.81				
15.63	87.5	104.3	47.3	0.67	0.80				
15.84	89.2	99.8	48.3	0.68	0.82				
15.99	89.1	104.2	48.2	0.67	0.81				
16.19	87.1	105.0	47.1	0.66	0.80				]]

Non-proprietary version

Table 25-5: Exposure Accounting Data for Plant B, Cycle 10

Cycle Expo. GWD/ST	Core Power % OLTP	Core Flow % Rated	Power Density kW/l	Avg. Core Exit Void Fract.	Max. Chan. Exit Void Fract.	MFLCPR	MFLPD	MAPRAT	Hot Critical Eigen-value
0.19	104.8	100.8	56.7	0.73	0.84	[[			
0.27	104.9	102.5	56.8	0.73	0.84				
0.44	104.6	100.2	56.6	0.73	0.84				
0.52	104.6	101.5	56.6	0.73	0.83				
0.80	104.7	98.8	56.7	0.74	0.84				
1.08	104.7	98.6	56.7	0.74	0.84				
1.36	104.7	98.4	56.7	0.74	0.84				
1.64	105.0	97.2	56.8	0.74	0.84				
1.88	105.0	96.7	56.8	0.74	0.84				
2.10	105.0	96.5	56.8	0.73	0.85				
2.25	104.9	97.3	56.7	0.73	0.85				
2.45	104.8	95.7	56.7	0.74	0.85				
2.52	87.8	105.0	47.5	0.68	0.79				
2.71	104.8	92.2	56.7	0.75	0.85				
2.82	104.3	104.2	56.4	0.72	0.83				
3.07	104.8	93.3	56.7	0.75	0.85				
3.32	104.9	93.3	56.8	0.75	0.85				
3.58	105.0	93.4	56.8	0.75	0.85				
3.83	105.0	92.3	56.8	0.75	0.85				
4.10	105.0	92.7	56.8	0.75	0.85				
4.18	104.9	99.9	56.8	0.73	0.84				
4.46	104.9	95.0	56.7	0.74	0.86				
4.73	104.9	96.0	56.7	0.74	0.85				
5.01	104.9	94.5	56.7	0.74	0.86				
5.16	104.8	94.5	56.7	0.74	0.86				
5.22	100.4	104.0	54.3	0.71	0.84				
5.50	104.9	94.6	56.7	0.74	0.86				
5.77	104.8	94.1	56.7	0.74	0.86				
6.05	105.0	93.7	56.8	0.74	0.86				
6.33	105.1	93.3	56.8	0.74	0.86				
6.61	105.0	92.9	56.8	0.74	0.87				
6.74	105.0	91.3	56.8	0.75	0.87				
6.80	98.6	104.5	53.3	0.70	0.85				
7.08	104.9	96.9	56.7	0.73	0.86				
7.36	104.9	96.2	56.7	0.73	0.87				
7.64	104.9	95.3	56.8	0.74	0.87				
7.92	105.0	95.3	56.8	0.74	0.87				

Non-proprietary version

Table 25-5: Exposure Accounting Data for Plant B, Cycle 10

Cycle Expo. GWD/ST	Core Power % OLTP	Core Flow % Rated	Power Density kW/l	Avg. Core Exit Void Fract.	Max. Chan. Exit Void Fract.	MFLCPR	MFLPD	MAPRAT	Hot Critical Eigen-value
8.20	104.8	94.0	56.7	0.74	0.87				
8.45	104.9	92.7	56.7	0.74	0.87				
8.68	105.0	92.3	56.8	0.74	0.88				
8.95	105.1	94.7	56.8	0.73	0.87				
9.23	104.8	94.9	56.7	0.73	0.87				
9.51	105.0	95.0	56.8	0.73	0.87				
9.79	105.0	94.8	56.8	0.73	0.87				
10.07	105.1	94.5	56.9	0.73	0.87				
10.30	105.1	93.8	56.8	0.74	0.87				
10.53	104.8	94.5	56.7	0.73	0.87				
10.76	105.0	94.8	56.8	0.73	0.87				
11.01	104.7	98.5	56.6	0.72	0.87				
11.24	104.9	99.6	56.8	0.72	0.86				
11.47	104.7	99.9	56.6	0.72	0.86				
11.53	104.7	95.3	56.6	0.73	0.87				
11.63	104.9	91.2	56.7	0.74	0.88				
11.80	104.8	95.7	56.7	0.73	0.87				
12.08	104.8	97.0	56.7	0.73	0.87				]]

Non-proprietary version

Table 25-6: Exposure Accounting Data for Plant C, Cycle 30

Cycle Expo. GWD/ST	Core Power % OLTP	Core Flow % Rated	Power Density kW/l	Avg. Core Exit Void Fract.	Max. Chan. Exit Void Fract.	MFLCPR	MFLPD	MAPRAT	Hot Critical Eigen-value
0.03	55.5	82.6	26.1	0.58	0.75	[[			
0.05	108.8	104.6	51.1	0.71	0.88				
0.12	109.5	115.3	51.5	0.70	0.86				
0.29	109.5	103.2	51.5	0.72	0.88				
0.43	109.8	105.6	51.6	0.71	0.88				
0.68	109.7	106.2	51.6	0.71	0.87				
0.94	109.7	106.1	51.6	0.71	0.87				
1.13	109.5	104.9	51.5	0.71	0.87				
1.43	109.6	104.0	51.5	0.72	0.88				
1.74	109.7	103.4	51.6	0.72	0.88				
1.85	109.7	101.6	51.6	0.72	0.89				
2.14	109.7	101.1	51.6	0.72	0.89				
2.25	109.8	100.8	51.6	0.72	0.89				
2.42	109.7	100.9	51.6	0.72	0.89				
2.53	109.7	100.7	51.6	0.72	0.89				
2.79	109.8	100.4	51.6	0.72	0.89				
3.05	109.4	100.4	51.4	0.72	0.89				
3.24	109.9	101.1	51.7	0.72	0.89				
3.33	109.6	101.8	51.5	0.72	0.87				
3.59	110.0	102.6	51.7	0.72	0.87				
3.72	109.7	104.1	51.6	0.71	0.87				
3.73	60.4	85.0	28.4	0.59	0.77				
3.75	109.4	117.2	51.4	0.69	0.86				
3.77	109.3	98.8	51.4	0.72	0.89				
3.84	109.7	95.3	51.6	0.73	0.90				
4.01	109.6	97.3	51.5	0.72	0.90				
4.22	109.6	98.4	51.5	0.72	0.90				
4.38	109.6	100.7	51.5	0.72	0.89				
4.55	109.6	103.0	51.5	0.71	0.89				
4.71	109.7	106.8	51.6	0.71	0.88				
4.87	109.8	108.3	51.6	0.70	0.88				
5.04	109.9	111.3	51.7	0.70	0.87				
5.18	109.9	114.1	51.7	0.69	0.87				
5.34	106.7	93.9	50.1	0.72	0.90				
5.50	106.0	93.9	49.8	0.72	0.89				
5.64	109.7	103.8	51.6	0.71	0.89				
5.85	109.6	108.8	51.5	0.70	0.88				

Non-proprietary version

Table 25-6: Exposure Accounting Data for Plant C, Cycle 30

Cycle Expo. GWD/ST	Core Power % OLTP	Core Flow % Rated	Power Density kW/l	Avg. Core Exit Void Fract.	Max. Chan. Exit Void Fract.	MFLCPR	MFLPD	MAPRAT	Hot Critical Eigen-value
6.06	108.9	113.7	51.2	0.69	0.87				
6.25	109.7	113.7	51.6	0.68	0.87				
6.34	109.7	113.4	51.6	0.68	0.87				
6.37	109.1	104.6	51.3	0.71	0.88				
6.39	98.8	104.6	46.4	0.68	0.86				
6.41	104.9	114.6	49.3	0.68	0.86				
6.43	106.1	116.0	49.9	0.68	0.86				
6.45	85.1	83.9	40.0	0.68	0.87				
6.48	93.5	93.8	43.9	0.68	0.87				
6.56	95.2	98.6	44.7	0.68	0.86				
6.69	105.3	114.6	49.5	0.67	0.86				
6.79	86.1	88.2	40.5	0.67	0.86				
6.85	97.8	114.0	46.0	0.66	0.84				
6.91	105.1	118.3	49.4	0.65	0.85				
7.07	103.4	119.0	48.6	0.65	0.84				
7.24	87.6	101.7	41.2	0.65	0.84				
7.31	80.7	89.3	37.9	0.65	0.84				
7.38	88.0	108.1	41.4	0.64	0.83				
7.48	91.9	118.5	43.2	0.63	0.82				
7.54	87.1	113.8	41.0	0.63	0.81				
7.60	73.4	82.4	34.5	0.64	0.83				]]

Non-proprietary version

Table 25-7: Exposure Accounting Data for Plant C, Cycle 31

Cycle Expo. GWD/ST	Core Power % OLTP	Core Flow % Rated	Power Density kW/l	Avg. Core Exit Void Fract.	Max. Chan. Exit Void Fract.	MFLCPR	MFLPD	MAPRAT	Hot Critical Eigen-value
0.01	48.4	70.3	22.8	0.58	0.74	[[			
0.02	53.9	82.6	25.3	0.59	0.74				
0.04	66.5	70.0	31.2	0.66	0.81				
0.06	109.5	95.7	51.5	0.74	0.89				
0.13	109.6	101.1	51.5	0.72	0.88				
0.27	109.9	103.3	51.7	0.72	0.88				
0.38	109.8	104.3	51.6	0.72	0.87				
0.50	103.4	94.2	48.6	0.72	0.88				
0.66	110.0	105.4	51.7	0.72	0.87				
0.82	109.9	105.4	51.7	0.72	0.87				
0.98	109.6	105.1	51.5	0.72	0.87				
1.15	109.7	104.5	51.6	0.72	0.87				
1.31	110.0	104.5	51.7	0.72	0.87				
1.47	109.9	104.2	51.7	0.72	0.87				
1.68	109.8	100.9	51.6	0.72	0.87				
1.89	109.8	100.4	51.6	0.72	0.87				
2.10	109.9	99.9	51.7	0.72	0.87				
2.31	109.7	99.2	51.6	0.72	0.87				
2.45	109.8	98.9	51.6	0.72	0.87				
2.61	110.1	98.9	51.8	0.72	0.87				
2.78	109.7	98.3	51.6	0.72	0.87				
2.94	109.6	98.2	51.5	0.72	0.87				
3.10	109.5	100.0	51.5	0.72	0.87				
3.26	109.8	100.0	51.6	0.73	0.87				
3.43	109.8	100.0	51.6	0.73	0.87				
3.59	109.9	100.3	51.7	0.72	0.87				
3.75	109.8	100.9	51.6	0.72	0.87				
3.92	110.1	102.1	51.8	0.72	0.87				
4.10	109.7	102.6	51.6	0.72	0.86				
4.29	109.3	103.8	51.4	0.72	0.86				
4.47	109.8	105.0	51.6	0.71	0.86				
4.61	109.6	98.0	51.5	0.72	0.88				
4.77	109.6	98.6	51.5	0.72	0.88				
4.94	109.7	100.2	51.6	0.72	0.88				
5.10	109.8	102.0	51.6	0.72	0.88				

Non-proprietary version

Table 25-7: Exposure Accounting Data for Plant C, Cycle 31

Cycle Expo. GWD/ST	Core Power % OLTP	Core Flow % Rated	Power Density kW/l	Avg. Core Exit Void Fract.	Max. Chan. Exit Void Fract.	MFLCPR	MFLPD	MAPRAT	Hot Critical Eigen-value
5.26	109.7	103.8	51.6	0.71	0.87				
5.38	109.7	106.7	51.6	0.71	0.87				
5.59	109.5	108.6	51.5	0.70	0.87				
5.70	109.9	111.6	51.7	0.70	0.86				
5.86	109.5	97.0	51.5	0.72	0.90				
6.07	109.5	99.2	51.5	0.72	0.89				
6.28	109.7	103.0	51.6	0.71	0.89				
6.49	109.8	107.6	51.6	0.70	0.88				
6.61	109.8	111.8	51.6	0.69	0.87				
6.72	109.6	116.4	51.5	0.68	0.86				
6.96	109.7	115.7	51.6	0.68	0.86				
7.16	109.9	117.1	51.7	0.67	0.86				
7.28	109.3	117.5	51.4	0.67	0.85				
7.39	108.2	117.8	50.8	0.66	0.85				
7.58	97.0	112.0	45.6	0.66	0.84				
7.67	103.8	118.3	48.8	0.65	0.84				
7.83	90.3	104.1	42.5	0.66	0.84				]]

Non-proprietary version

Table 25-8: Exposure Accounting Data for Plant D, Cycle 15

Cycle Expo. GWD/ST	Core Power % OLTP	Core Flow % Rated	Power Density kW/l	Avg. Core Exit Void Fract.	Max. Chan. Exit Void Fract.	MFLCPR	MFLPD	MAPRAT	Hot Critical Eigen-value
0.35	119.9	103.2	59.0	0.75	0.84	[[			
0.62	119.9	103.1	58.9	0.75	0.84				
0.88	120.1	101.4	59.0	0.75	0.84				
1.15	120.0	101.3	59.0	0.76	0.84				
1.41	120.2	104.1	59.1	0.75	0.84				
1.73	120.0	101.6	59.0	0.76	0.84				
1.87	120.0	103.8	59.0	0.75	0.83				
2.11	119.9	101.5	59.0	0.76	0.84				
2.38	119.8	99.6	58.9	0.76	0.84				
2.64	119.7	99.9	58.9	0.76	0.84				
2.83	119.9	102.2	59.0	0.75	0.84				
2.97	120.0	103.3	59.0	0.75	0.84				
3.23	119.6	102.1	58.8	0.75	0.84				
3.40	119.9	101.5	59.0	0.76	0.84				
3.59	119.9	103.0	58.9	0.75	0.84				
3.86	120.0	103.0	59.0	0.75	0.84				
4.12	119.8	101.6	58.9	0.76	0.84				
4.39	119.9	101.1	58.9	0.76	0.84				
4.65	120.1	99.9	59.1	0.76	0.85				
4.85	120.1	101.1	59.1	0.76	0.85				
5.12	120.0	101.8	59.0	0.76	0.84				
5.25	119.8	100.5	58.9	0.76	0.85				
5.38	119.9	102.1	58.9	0.75	0.85				
5.64	119.7	100.9	58.9	0.76	0.85				
5.91	120.1	103.2	59.0	0.75	0.85				
6.17	120.0	103.0	59.0	0.75	0.85				
6.44	119.9	101.4	58.9	0.76	0.86				
6.73	120.0	103.0	59.0	0.75	0.86				
6.99	120.1	102.1	59.1	0.75	0.86				]]

Non-proprietary version

Table 25-9: Exposure Accounting Data for Plant E, Cycle 9

Cycle Expo. GWD/ST	Core Power % OLTP	Core Flow % Rated	Power Density kW/l	Avg. Core Exit Void Fract.	Max. Chan. Exit Void Fract.	MFLCPR	MFLPD	MAPRAT	Hot Critical Eigen-value
0.28	111.1	92.5	58.2	0.75	0.87	[[			
0.58	111.0	97.8	58.2	0.74	0.86				
0.89	111.3	97.9	58.3	0.74	0.86				
1.16	113.3	98.2	59.4	0.75	0.86				
1.38	113.8	98.1	59.6	0.75	0.86				
1.64	113.4	93.7	59.4	0.76	0.87				
1.85	113.6	93.7	59.5	0.76	0.87				
2.06	113.4	95.8	59.4	0.75	0.86				
2.33	113.5	95.2	59.5	0.76	0.86				
2.60	113.5	94.8	59.5	0.76	0.86				
2.89	113.3	96.0	59.4	0.75	0.86				
3.08	112.7	93.1	59.1	0.76	0.87				
3.34	112.6	93.5	59.0	0.76	0.86				
3.60	111.7	92.6	58.5	0.76	0.86				
3.91	111.5	94.0	58.5	0.76	0.86				
4.23	111.1	92.6	58.2	0.76	0.86				
4.54	109.8	91.0	57.6	0.76	0.87				
4.82	109.5	92.3	57.4	0.75	0.86				
5.11	109.7	91.2	57.5	0.76	0.87				
5.26	109.5	90.6	57.4	0.76	0.87				
5.42	109.5	90.2	57.4	0.76	0.87				
5.66	109.5	91.1	57.4	0.76	0.87				
5.96	109.6	89.8	57.4	0.76	0.87				
6.14	109.4	91.2	57.4	0.76	0.87				
6.32	109.6	89.5	57.4	0.76	0.87				
6.59	109.3	95.3	57.3	0.75	0.86				
6.85	109.3	93.5	57.3	0.75	0.87				
7.06	109.3	92.1	57.3	0.76	0.87				
7.24	109.5	91.3	57.4	0.76	0.87				
7.39	109.6	92.4	57.4	0.76	0.87				
7.54	109.3	91.7	57.3	0.76	0.87				
7.70	109.4	90.1	57.3	0.76	0.87				
7.90	109.4	92.5	57.3	0.76	0.87				
8.11	109.1	90.4	57.2	0.76	0.87				
8.34	109.2	90.6	57.2	0.76	0.87				

Non-proprietary version

Table 25-9: Exposure Accounting Data for Plant E, Cycle 9

Cycle Expo. GWD/ST	Core Power % OLTP	Core Flow % Rated	Power Density kW/l	Avg. Core Exit Void Fract.	Max. Chan. Exit Void Fract.	MFLCPR	MFLPD	MAPRAT	Hot Critical Eigen-value
8.47	109.3	91.6	57.3	0.76	0.87				
8.62	109.2	91.2	57.2	0.76	0.87				
8.76	109.1	93.1	57.2	0.75	0.87				
8.94	109.1	92.9	57.2	0.75	0.87				
9.01	109.2	93.0	57.2	0.75	0.87				
9.14	109.4	93.0	57.3	0.75	0.87				
9.30	109.6	92.2	57.5	0.76	0.87				
9.48	109.6	91.9	57.4	0.76	0.87				
9.62	109.6	93.2	57.4	0.76	0.87				
9.83	111.6	93.7	58.5	0.76	0.87				
10.02	111.1	93.2	58.2	0.76	0.87				
10.20	111.5	93.7	58.4	0.76	0.87				
10.28	111.8	94.9	58.6	0.76	0.87				
10.54	111.9	95.3	58.7	0.76	0.86				
10.78	111.5	95.2	58.5	0.76	0.86				
10.94	112.1	97.0	58.8	0.76	0.86				
11.12	112.0	95.0	58.7	0.76	0.86				
11.30	111.9	95.3	58.6	0.76	0.86				
11.49	112.4	94.8	58.9	0.76	0.86				
11.62	112.1	93.4	58.8	0.76	0.87				
11.70	112.1	96.4	58.8	0.75	0.87				
11.86	112.2	95.2	58.8	0.76	0.86				
12.07	112.4	94.9	58.9	0.76	0.86				
12.23	112.4	97.1	58.9	0.76	0.86				
12.31	111.8	93.3	58.6	0.76	0.86				
12.44	111.6	96.3	58.5	0.76	0.86				
12.49	109.1	96.9	57.2	0.75	0.86				
12.77	109.5	94.0	57.4	0.75	0.86				
12.95	109.3	93.1	57.3	0.76	0.86				
13.13	108.9	92.5	57.1	0.76	0.86				
13.31	108.9	92.6	57.1	0.76	0.86				
13.49	108.9	95.3	57.1	0.75	0.85				
13.74	109.0	94.6	57.1	0.75	0.85				
13.83	111.4	99.1	58.4	0.75	0.85				
14.14	111.5	98.7	58.4	0.75	0.85				
14.43	110.0	102.6	57.6	0.74	0.83				
14.62	107.2	103.0	56.2	0.73	0.83				

Non-proprietary version

Table 25-9: Exposure Accounting Data for Plant E, Cycle 9

Cycle Expo. GWD/ST	Core Power % OLTP	Core Flow % Rated	Power Density kW/l	Avg. Core Exit Void Fract.	Max. Chan. Exit Void Fract.	MFLCPR	MFLPD	MAPRAT	Hot Critical Eigen-value
14.84	105.1	103.4	55.1	0.73	0.82				
14.93	103.5	103.8	54.2	0.72	0.82				
15.20	105.1	103.9	55.1	0.72	0.81				
15.49	101.1	102.9	53.0	0.71	0.81				
15.76	97.7	105.0	51.2	0.70	0.79				
15.98	93.7	105.6	49.1	0.68	0.78				]]

Non-proprietary version

Table 25-10: Exposure Accounting Data for Plant E, Cycle 10

Cycle Expo. GWD/ST	Core Power % OLTP	Core Flow % Rated	Power Density kW/l	Avg. Core Exit Void Fract.	Max. Chan. Exit Void Fract.	MFLCPR	MFLPD	MAPRAT	Hot Critical Eigen-value
0.17	111.1	95.5	58.2	0.76	0.84	[[			
0.36	111.5	100.5	58.5	0.75	0.83				
0.54	111.5	98.2	58.4	0.76	0.84				
0.61	111.5	97.9	58.4	0.76	0.84				
0.91	111.2	95.6	58.3	0.76	0.84				
1.19	111.3	95.0	58.3	0.76	0.84				
1.49	113.3	97.7	59.4	0.76	0.84				
1.78	113.6	97.2	59.6	0.76	0.85				
1.84	57.7	75.0	30.2	0.63	0.79				
2.08	114.1	94.9	59.8	0.77	0.85				
2.32	113.8	95.8	59.7	0.76	0.85				
2.56	114.4	96.3	60.0	0.77	0.85				
2.83	114.0	94.0	59.8	0.77	0.86				
2.91	114.1	94.4	59.8	0.77	0.85				
3.13	114.1	94.1	59.8	0.77	0.86				
3.34	114.3	94.7	59.9	0.77	0.86				
3.39	114.5	97.1	60.0	0.76	0.85				
3.65	114.4	96.4	59.9	0.77	0.86				
3.92	114.3	97.1	59.9	0.76	0.86				
4.19	114.5	96.6	60.0	0.77	0.86				
4.45	114.5	95.7	60.0	0.77	0.86				
4.56	114.4	96.0	59.9	0.77	0.86				]]

Non-proprietary version

Table 25-11. Cold Critical Eigenvalues for All Studied Cycles

Plant, Cycle	Cycle Exposure GWD/ST	Measured Cold Critical Eigenvalue	Nuclear Design Basis Cold Critical Eigenvalue
Plant A. C18	0.00	[[	
	3.04		
	6.13		
	7.85		
	9.68		
	13.58		
Plant A. C19	0.00		
	4.80		
	4.87		
	4.88		
Plant B. C9	0.00		
	11.86		
Plant B. C10	0.00		
	0.00		
	8.68		
Plant C. C30	0.00		
	0.00		
	0.00		
	0.00		
	6.34		
	7.60		
	7.60		
	7.60		
	7.60		
Plant C. C31	0.00		
	0.00		
	0.00		
	0.00		
	0.00		
	0.00		
	0.00		
	0.00		
	0.00		
	7.83		
	7.83		
	7.83		
	7.83		
Plant D. C15	0.00		
	3.4		
Plant E. C 9	0.00		
Plant E. C 10	0		
	3.4		]]

NOTE: PANAC10 was used to design both of these cycles, using PANAC10-based eigenvalues for the Nuclear Design Basis. The tests, however were evaluated with PANAC11, for which there were no Nuclear Design Basis eigenvalues defined.

Non-proprietary version

Table 25-12. TIP Comparisons for the Studied Cycles

Cycle Expo. GWD/ST	Core Power %OLTP	Core Flow % Rated	Bundle RMS %	Axial RMS %	Nodal RMS %	Avg. Core Exit Void Fract.	Max Chan. Exit Void Fract.	MFLCPR	MFLPD	MAPRAT
Plant A – Cycle 18										
2.34	104.0	93.6	]]			0.74	0.84	]]		
3.37	103.4	94.2				0.73	0.84			
4.18	112.2	94.4			]]	0.75	0.86			]]
Plant A – Cycle 19										
0.24	112.4	94.8	]]			0.76	0.83	]]		
1.17	112.5	92.8				0.76	0.83			
2.13	112.4	94.3				0.76	0.84			
2.50	112.3	95.4				0.75	0.85			
3.16	112.3	96.9				0.75	0.85			
4.19	112.5	93.6				0.76	0.86			
4.51	112.2	97.6				0.75	0.84			
5.18	112.5	97.9				0.75	0.84			
6.26	112.3	94.4				0.76	0.85			
7.22	112.4	94.4				0.75	0.86			
8.13	112.6	94.3				0.75	0.86			
9.02	112.6	96.0			]]	0.75	0.86			]]
Plant B – Cycle 9										
0.26	104.8	99.4	]]			0.74	0.83	]]		
0.54	104.9	90.6				0.76	0.84			
0.79	104.9	91.1				0.76	0.84			
1.42	104.8	96.9				0.74	0.83			
1.61	105.0	94.9				0.75	0.84			
2.20	104.6	89.7				0.76	0.85			
2.50	104.9	89.7				0.76	0.86			
3.41	104.6	85.7				0.76	0.87			
3.87	104.6	85.0				0.76	0.87			
4.39	105.0	92.1				0.75	0.86			
5.92	104.7	87.6				0.76	0.86			
6.92	105.1	86.4				0.76	0.87			
7.20	105.0	98.0				0.74	0.86			
7.76	104.9	95.5				0.74	0.86			
8.49	105.0	92.9				0.75	0.87			
9.20	105.0	91.0				0.75	0.87			
9.58	96.8	103.9				0.70	0.82			

Non-proprietary version

Table 25-12. TIP Comparisons for the Studied Cycles

Cycle Expo. GWD/ST	Core Power %OLTP	Core Flow % Rated	Bundle RMS %	Axial RMS %	Nodal RMS %	Avg. Core Exit Void Fract.	Max Chan. Exit Void Fract.	MFLCPR	MFLPD	MAPRAT
10.06	105.1	100.6				0.73	0.85			
10.34	104.8	99.6				0.73	0.85			
11.12	105.1	99.5				0.73	0.85			
12.00	101.1	103.3				0.71	0.85			
13.21	104.6	101.3				0.72	0.85			
13.71	104.8	93.1				0.74	0.87			
14.24	104.9	97.2				0.73	0.86			
14.49	104.1	102.9				0.72	0.84			
14.76	104.6	102.1				0.72	0.85			
15.21	102.8	104.1				0.71	0.84			
15.63	88.1	103.5				0.67	0.81			
15.99	89.2	103.6			]]	0.67	0.81			]]
Plant B – Cycle 10										
0.19	94.1	102.7	]]			0.70	0.80	]]		
0.27	104.5	102.1				0.73	0.83			
0.80	105.0	98.1				0.74	0.84			
1.64	104.9	96.9				0.74	0.84			
2.45	105.0	96.7				0.74	0.85			
4.10	104.9	92.3				0.75	0.85			
4.18	105.0	92.6				0.75	0.85			
4.46	104.9	95.6				0.74	0.85			
5.01	104.9	95.5				0.74	0.86			
5.77	104.9	94.0				0.74	0.86			
6.61	104.9	93.0				0.74	0.87			
7.08	104.8	97.4				0.73	0.86			
7.92	104.9	95.4				0.74	0.87			
8.20	105.1	95.4				0.74	0.87			
8.68	105.0	92.3			]]	0.74	0.88			]]
Plant C – Cycle 30										
0.43	110.0	98.2	]]			0.71	0.88	]]		
1.13	109.8	97.7				0.71	0.87			
1.85	109.8	94.7				0.71	0.88			
2.25	109.5	93.8				0.72	0.89			
2.53	109.8	93.4				0.72	0.89			
3.33	109.7	94.5				0.72	0.87			
3.84	109.9	88.6				0.73	0.90			
4.01	109.9	90.2				0.73	0.90			

Non-proprietary version

Table 25-12. TIP Comparisons for the Studied Cycles

Cycle Expo. GWD/ST	Core Power %OLTP	Core Flow % Rated	Bundle RMS %	Axial RMS %	Nodal RMS %	Avg. Core Exit Void Fract.	Max Chan. Exit Void Fract.	MFLCPR	MFLPD	MAPRAT
4.71	109.5	98.9				0.71	0.88			
5.34	106.7	87.0				0.72	0.90			
6.25	109.5	105.7				0.68	0.87			
6.48	94.3	88.5				0.68	0.87			
6.91	105.1	109.8				0.65	0.85			
0.50	103.7	87.7				0.72	0.88			
0.98	110.2	97.8				0.72	0.87			
1.68	110.0	93.7				0.72	0.87			
2.45	109.9	92.3				0.72	0.87			
3.10	109.7	93.0				0.72	0.87			
3.92	109.9	94.8				0.72	0.87			
4.61	109.6	90.9				0.72	0.88			
5.38	109.6	99.1				0.71	0.87			
5.86	109.7	90.1				0.72	0.90			
6.72	109.5	107.8				0.68	0.86			
7.28	109.3	109.2			]]	0.66	0.85			]]
Plant E – Cycle 9										
0.25	111.1	92.6	[[			0.75	0.87	[[		
0.51	111.2	98.2				0.74	0.86			
3.72	111.7	94.0				0.76	0.86			
3.77	111.6	94.7				0.75	0.86			
4.78	109.8	92.5				0.75	0.86			
5.69	109.5	90.9				0.76	0.87			
7.54	109.3	90.8				0.76	0.87			
9.31	109.5	92.5				0.76	0.87			
10.20	111.5	93.7				0.76	0.87			
11.03	112.0	94.6				0.76	0.87			
11.98	112.2	95.0				0.76	0.86			
12.91	109.0	94.0				0.75	0.86			
14.62	106.0	103.2				0.73	0.82			
15.40	100.8	104.3			]]	0.70	0.80			]]
Plant E – Cycle 10										
0.14	111.7	95.4	[[			0.76	0.84	[[		
0.79	111.0	93.9				0.76	0.84			
1.71	113.5	95.6				0.77	0.85			
2.47	114.6	96.6				0.76	0.85			
3.58	114.2	96.2				0.77	0.86			

Non-proprietary version

Table 25-12. TIP Comparisons for the Studied Cycles

Cycle Expo. GWD/ST	Core Power %OLTP	Core Flow % Rated	Bundle RMS %	Axial RMS %	Nodal RMS %	Avg. Core Exit Void Fract.	Max Chan. Exit Void Fract.	MFLCPR	MFLPD	MAPRAT
5.73	113.8	97.5				0.76	0.85			
6.58	113.3	96.6				0.76	0.85			
7.38	113.9	95.9				0.77	0.86			
8.45	110.8	95.8			]]	0.76	0.86			]]

Non-proprietary version

Table 25-13: Exposure Accounting Data for Plant E, Cycle 8

Cycle Expo.	Core Power	Core Flow	Power Density	Power/Flow Ratio	Hot Critical Eigenvalue
GWD/ST	% OLTP	% Rated	kW/l	MWt/Mlbm/hr	
0.24	99.9	92.8	52.3	36.8	[[
0.47	100.0	96.6	52.4	35.4	
0.63	100.0	90.1	52.4	38.0	
0.84	100.0	89.9	52.4	38.1	
1.05	99.9	88.8	52.4	38.6	
1.19	100.1	90.1	52.5	38.0	
1.38	100.0	90.5	52.4	37.8	
1.57	99.9	90.9	52.4	37.7	
1.73	99.8	90.6	52.3	37.7	
1.85	99.9	91.1	52.4	37.6	
1.90	99.8	100.5	52.3	34.0	
2.08	99.7	83.7	52.3	40.8	
2.22	100.1	90.1	52.5	38.0	
2.34	100.0	95.0	52.4	36.0	
2.43	100.0	100.0	52.4	34.3	
2.77	99.9	92.6	52.4	37.0	
2.95	100.0	93.1	52.4	36.8	
3.26	100.0	93.6	52.4	36.6	
3.54	100.0	94.3	52.4	36.3	
3.75	99.9	94.7	52.4	36.1	
3.92	99.9	95.2	52.4	36.0	
4.06	99.9	94.9	52.4	36.1	
4.25	100.0	94.9	52.4	36.1	
4.39	100.0	95.0	52.4	36.1	
4.58	99.9	89.3	52.4	38.3	
4.79	100.0	89.5	52.4	38.3	
5.09	100.0	89.8	52.4	38.1	
5.40	100.0	88.7	52.4	38.6	
5.71	100.0	88.8	52.4	38.6	
5.95	100.1	87.2	52.5	39.3	
6.23	99.9	87.1	52.4	39.3	
6.51	99.9	86.6	52.4	39.5	
6.61	99.9	89.9	52.4	38.1	
6.70	99.6	91.5	52.2	37.3	
6.89	99.5	95.8	52.2	35.6	

Non-proprietary version

Table 25-13: Exposure Accounting Data for Plant E, Cycle 8

Cycle Expo.	Core Power	Core Flow	Power Density	Power/Flow Ratio	Hot Critical Eigenvalue
GWD/ST	% OLTP	% Rated	kW/l	MWt/Mlbm/hr	
7.10	100.0	96.0	52.4	35.6	
7.38	100.0	89.8	52.4	38.1	
7.66	99.6	89.9	52.2	37.9	
7.92	100.0	90.6	52.4	37.8	
8.18	100.0	90.8	52.4	37.7	
8.46	99.9	94.6	52.4	36.2	
8.65	100.0	93.0	52.4	36.8	
8.84	99.9	93.2	52.4	36.7	
9.06	99.9	93.4	52.4	36.6	
9.21	99.9	93.0	52.4	36.8	
9.35	99.9	96.3	52.4	35.6	
9.59	100.0	94.6	52.4	36.2	
9.84	100.0	95.3	52.4	36.0	
10.10	100.0	94.9	52.4	36.1	
10.33	100.0	94.6	52.4	36.2	
10.50	99.8	98.5	52.3	34.7	
10.78	99.9	89.4	52.3	38.3	
11.04	99.9	97.1	52.4	35.2	
11.13	98.9	100.2	51.8	33.8	
11.23	100.1	99.3	52.5	34.5	
11.39	98.5	100.1	51.6	33.7	
11.53	96.1	100.2	50.4	32.8	]]

Table 25-14. Summary of Bundle Average TIP Comparisons, Eight Cycles Studied

Document	Nuclear Model	# of TIP Sets	Weighted RMS Difference
NEDE-32694 (used in SLMCPR Analysis)	TGBLA04/PANAC10	[[	
NEDE-32773-R1 (Jan 1999)	TGBLA06/PANAC11		
Current data from Eight Cycles Studied	TGBLA06/PANAC11		]]

Non-proprietary version

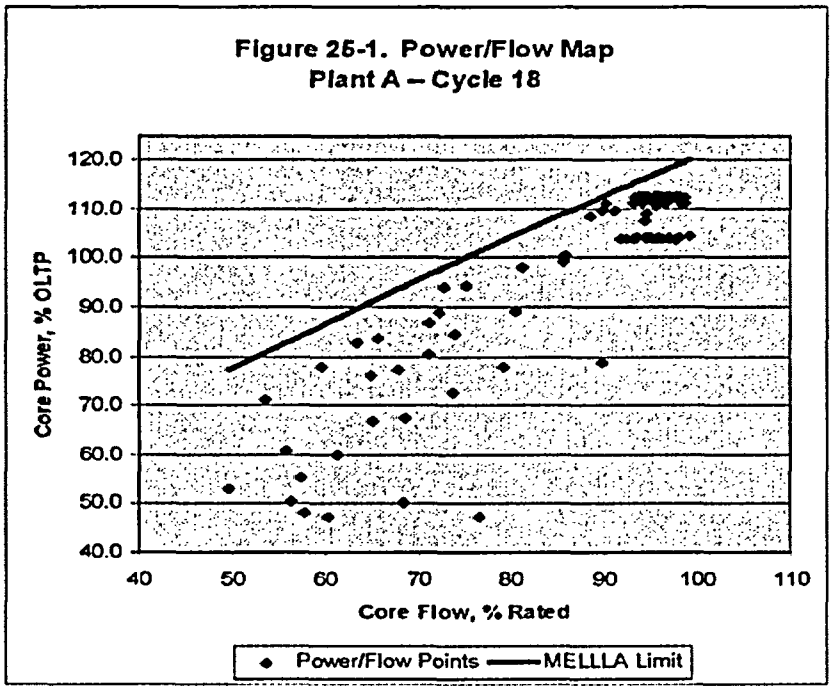

Non-proprietary version

Figure 25-2. Core Power/Flow Map
Plant A – Cycle 19

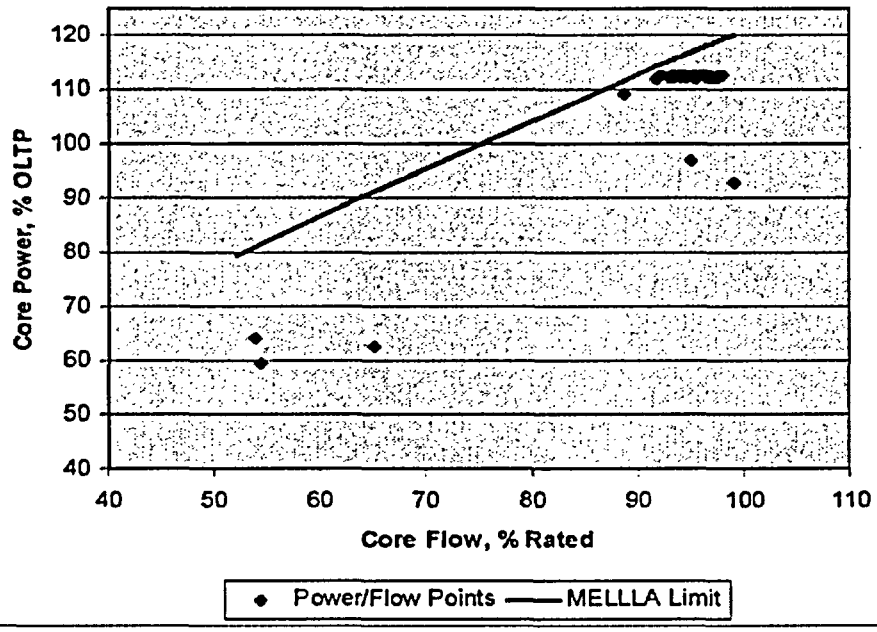

Non-proprietary version

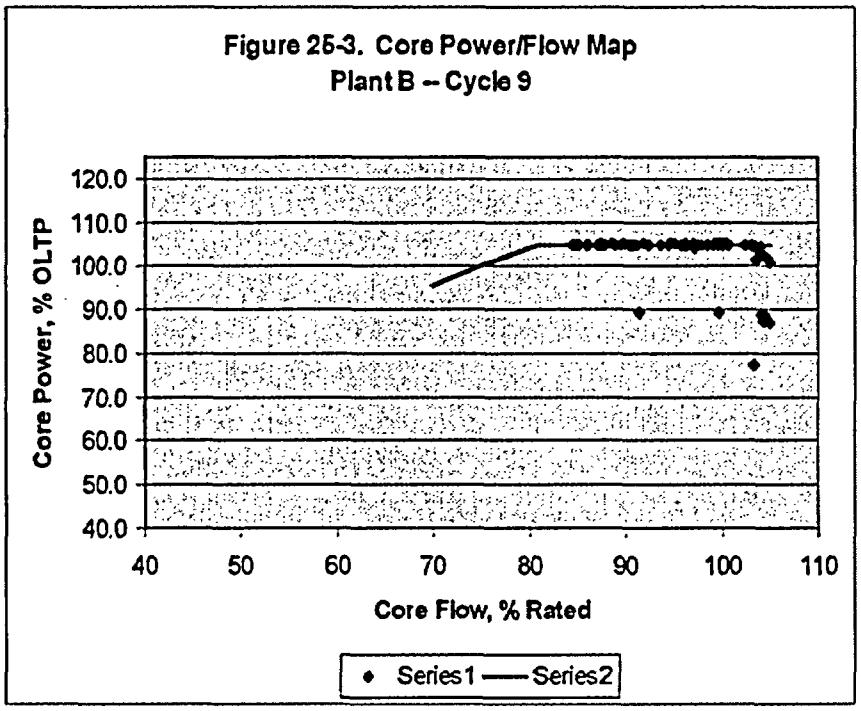

Figure 25-4. Core Power/Flow Map
Plant B – Cycle 10

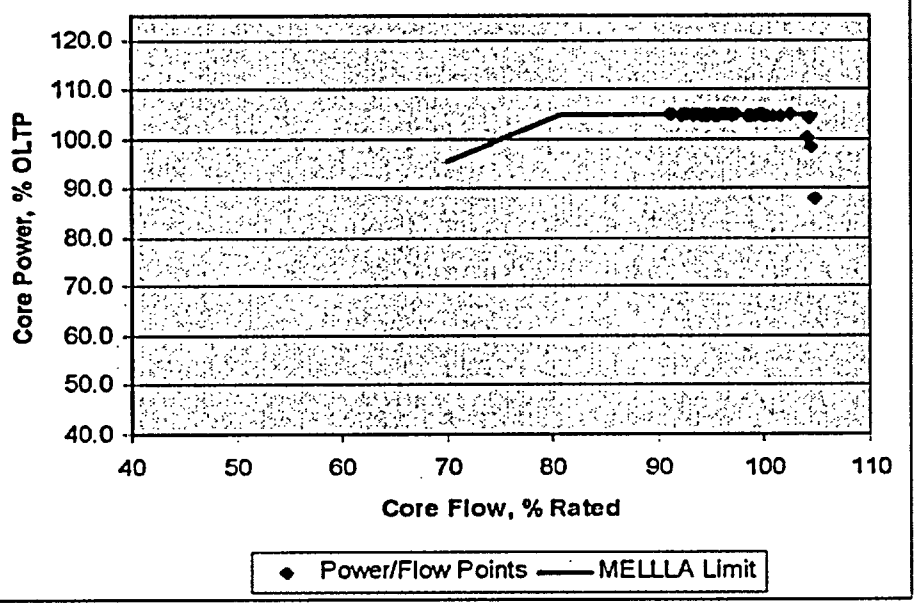

Non-proprietary version

Figure 25-5. Core Power/Flow Map
Plant C -- Cycle 30

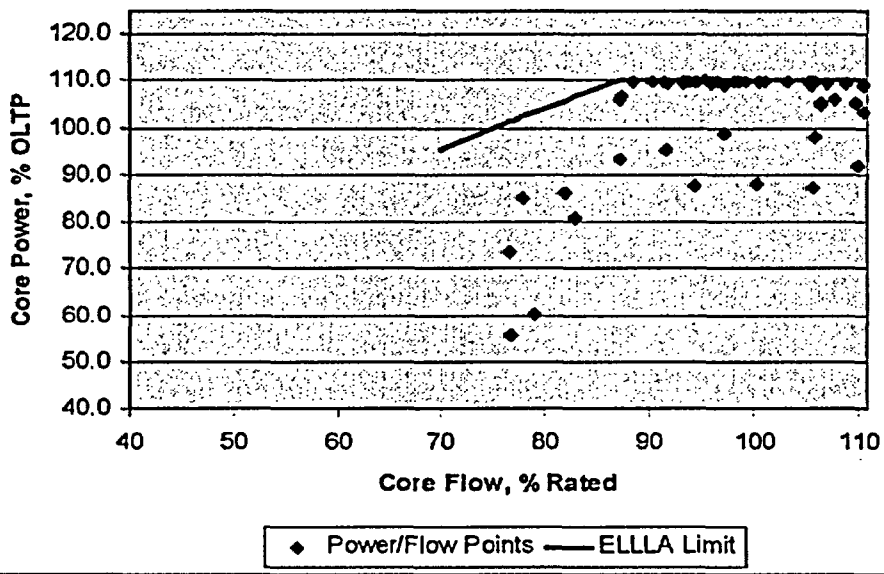

Non-proprietary version

Figure 25-6. Core Power/Flow Map
Plant C – Cycle 31

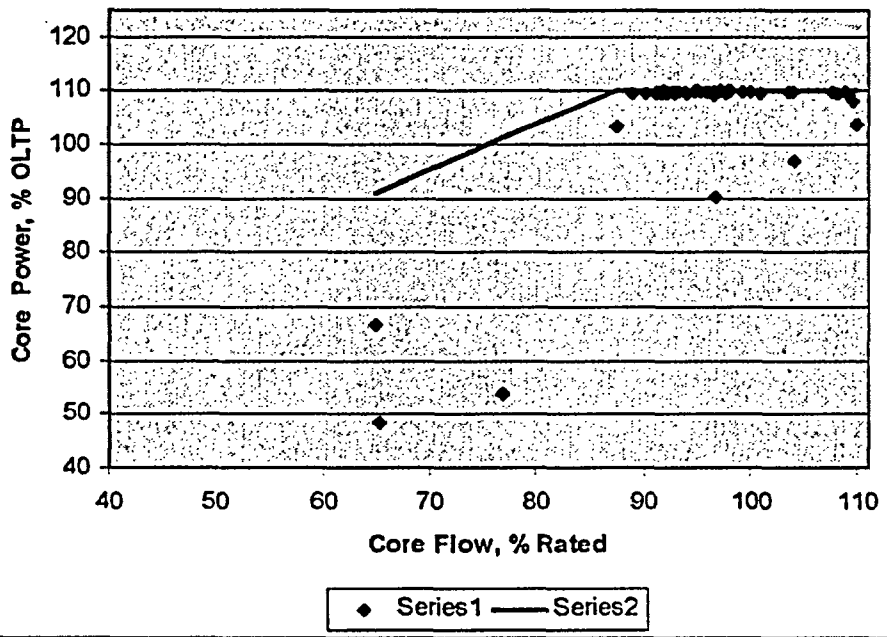

Figure 25-7. Core Power/Flow Map
Plant D – Cycle 15

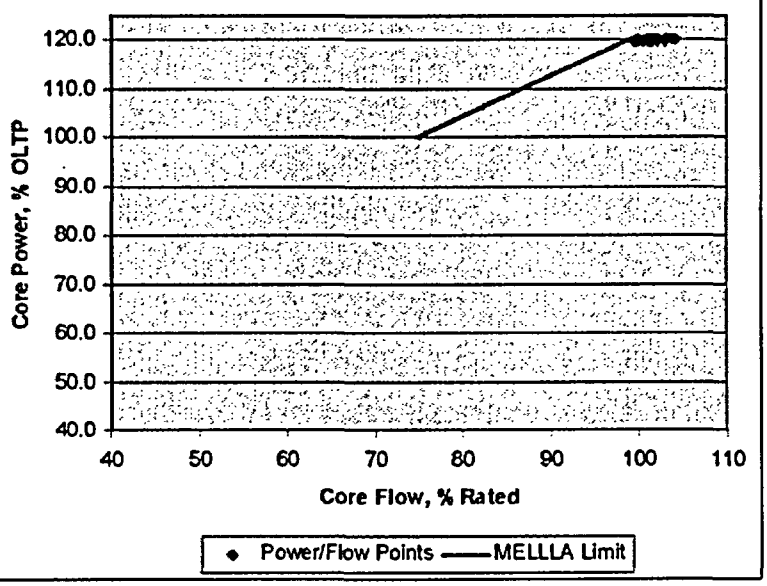

Figure 25-8. Power Flow Map
Plant E – Cycle 9

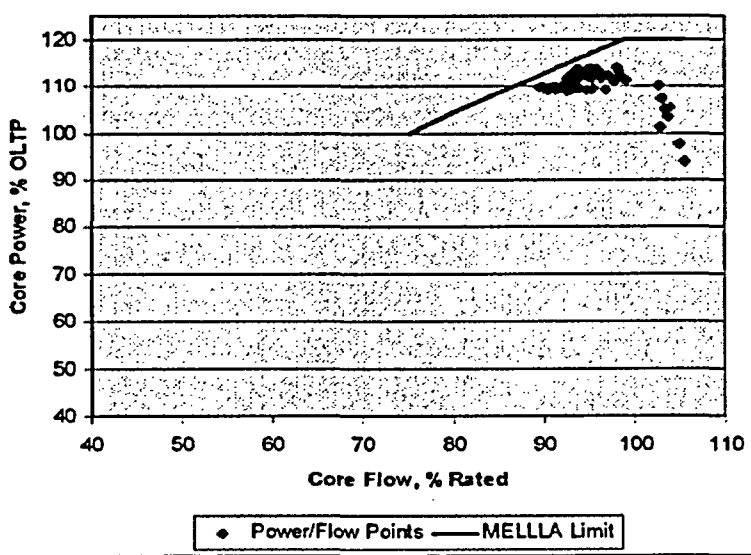

Non-proprietary version

Figure 25-9. Power/Flow Map
Plant E -- Cycle 10

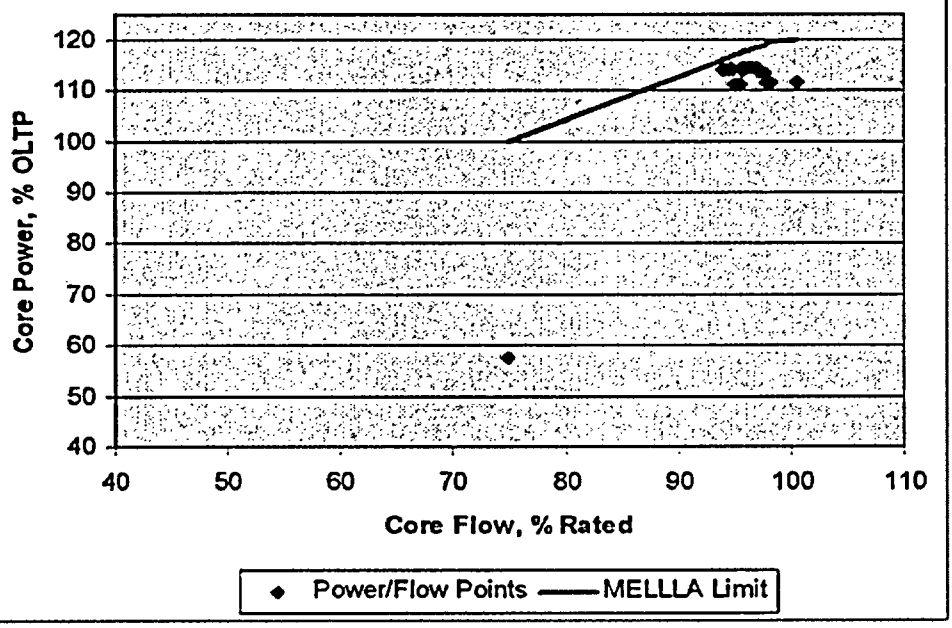

Non-proprietary version

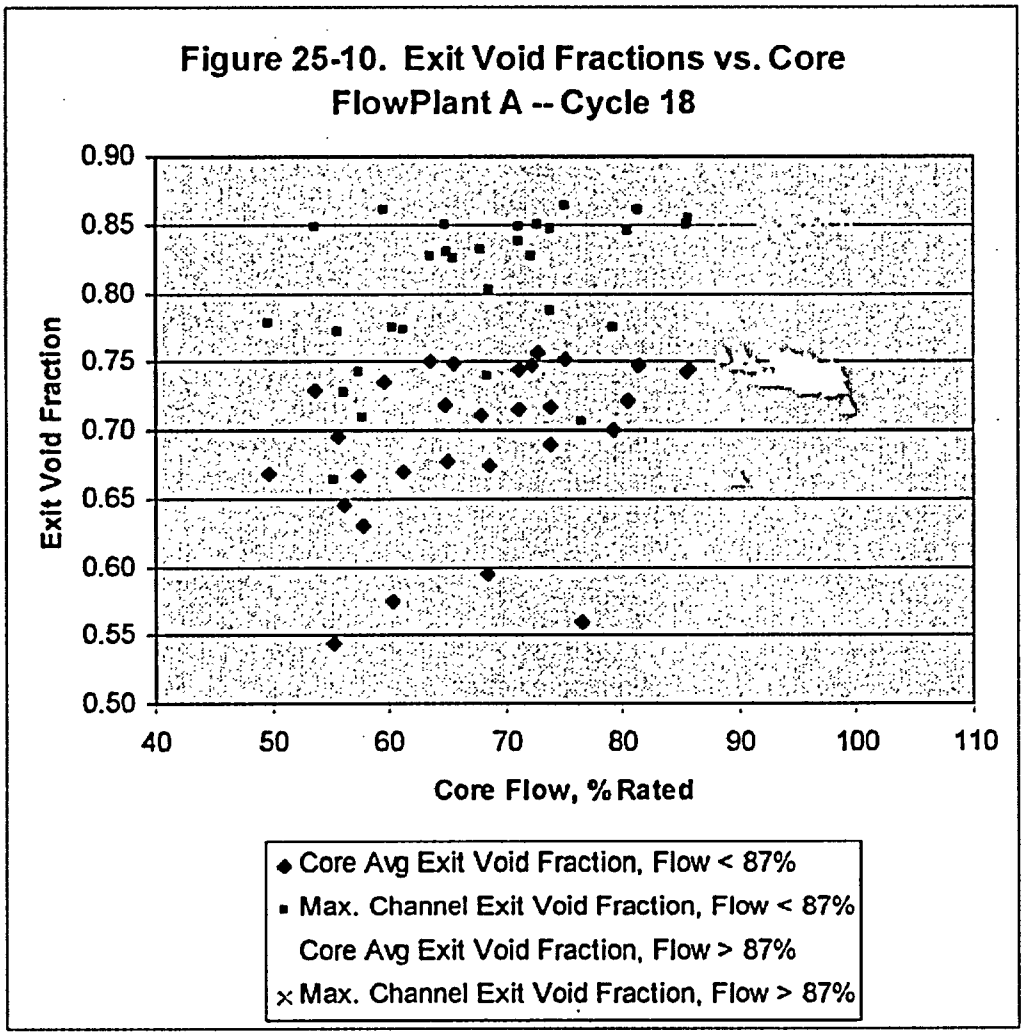

[[

]]

Non-proprietary version

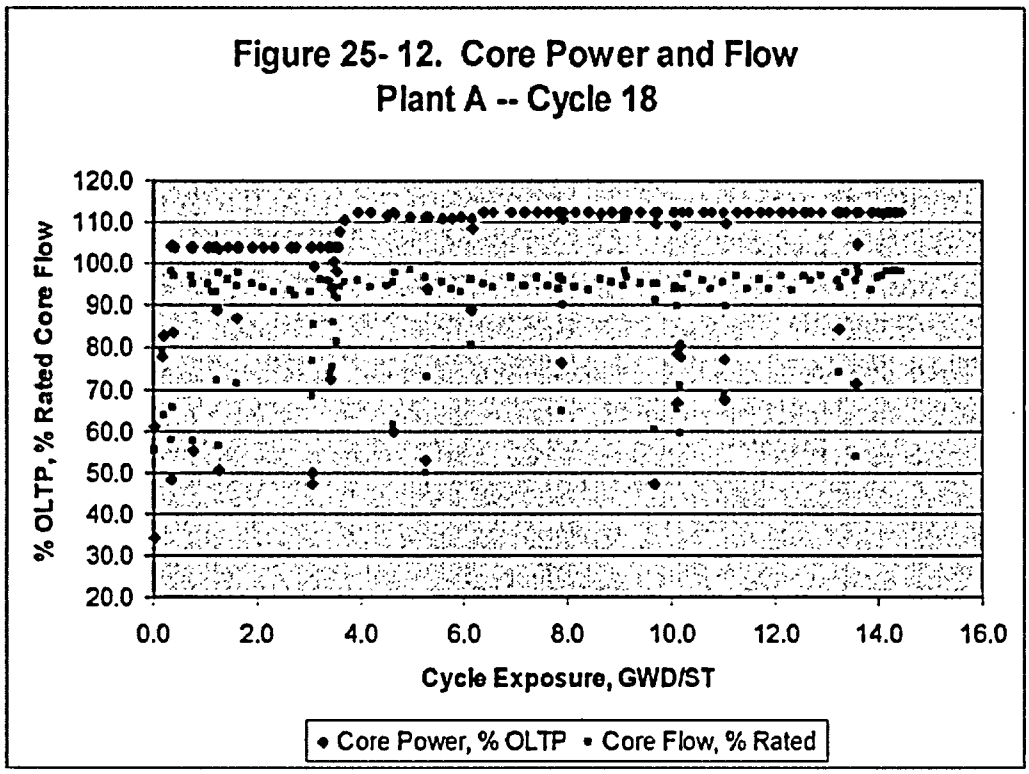

Non-proprietary version

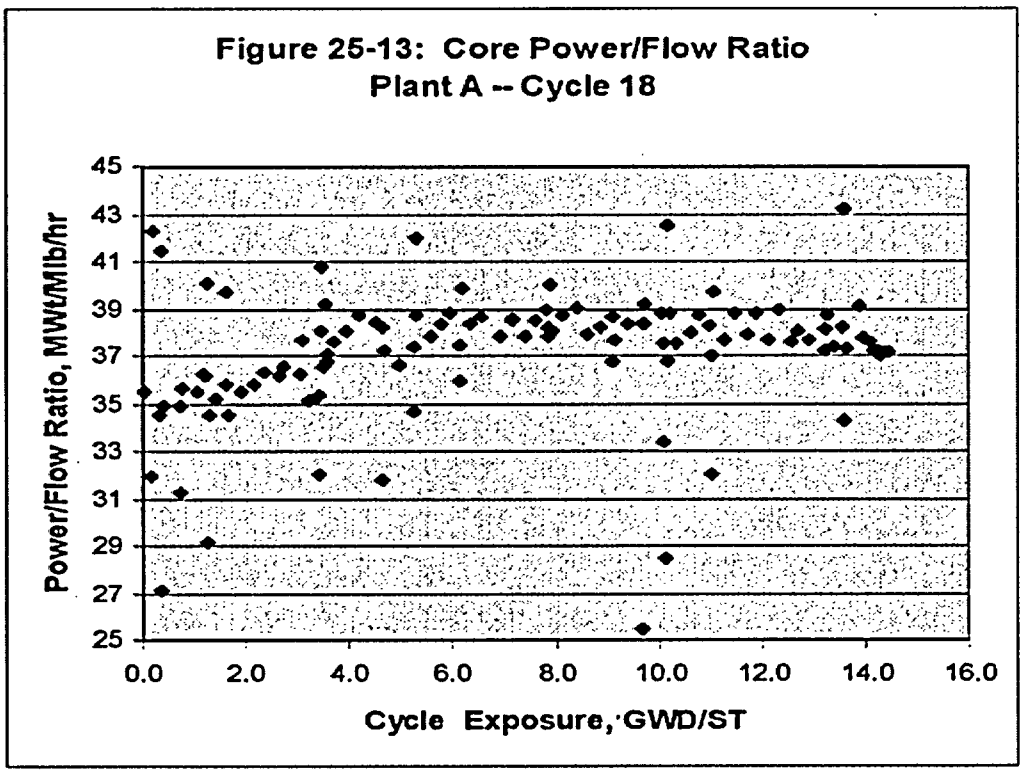

Non-proprietary version

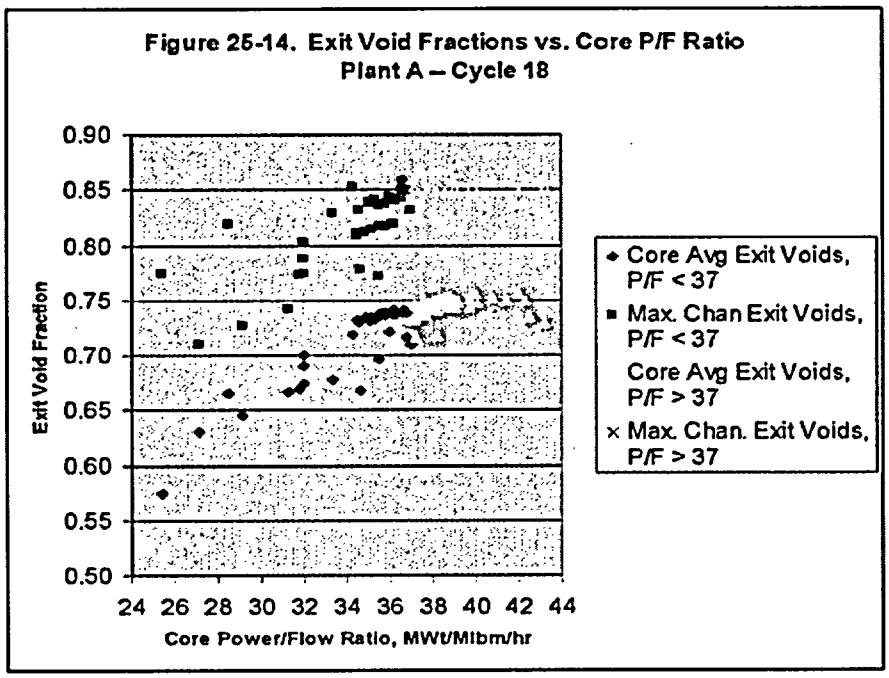

[[

]]

Non-proprietary version

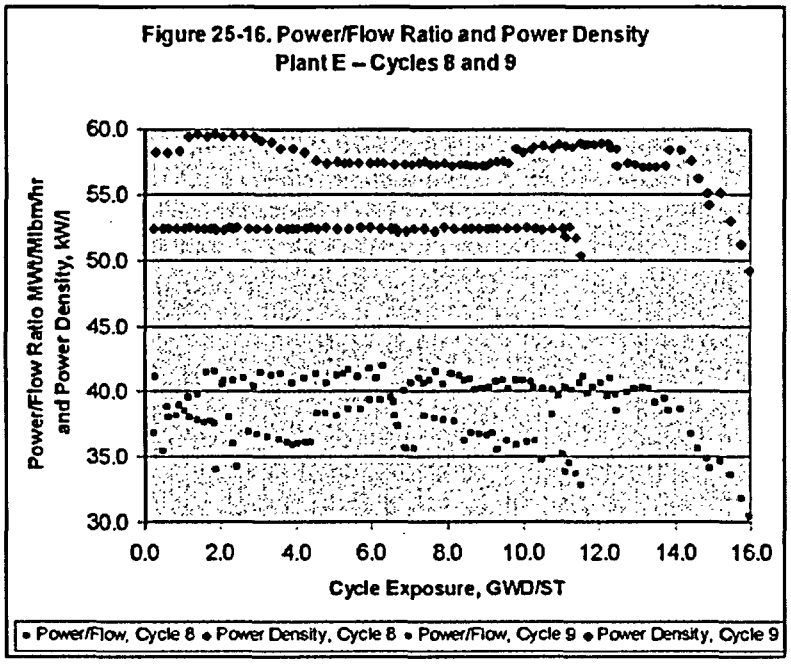

[[

]]

[[

]]

[[

]]

[[

]]

NRC RAI 26

Low-Flow and Off-rated Conditions: BWRs currently operate with lower core flow ranges at rated power. However, the general practice is to benchmark the codes for plant operation at rated conditions on the assumption that plants do not routinely operate at the lower flow conditions. The low-flow conditions can be limiting for the thermal-hydraulic conditions (e.g., higher void conditions, axial and radial power peaking and distribution) that adversely affect the performance of the core and the fuel (critical power ratio response). As far as the available data allows, include core follow data for nonrated conditions. If core follow data during plant maneuvers (i.e., during startup, off-rated, and lower core flow at rated power operation) is not available, provide a commitment to benchmark the fidelity of your lattice physics and core simulator codes at these conditions for the EPU/MELLLA+ operation. State what actions you will take to fulfill this commitment.

GE Response to RAI 26

As stated in RAI 26, BWRs currently operate with lower core flow ranges at rated power. This statement is corroborated by the Power Flow Maps provided in the response to RAI 25 in Figures 25-1 through 25-9. Because the plants operate at steady state over these flow ranges at high power, these state points are included in the normal exposure accounting calculations for core tracking. Generally, off-rated conditions such as those on the plant's startup trajectory, or during control rod sequence exchanges, are not included in the core tracking because the core is not in an equilibrium state at these conditions due to transient xenon effects.

The exposure accounting data that was evaluated in the response to RAI 25 included a large number of statepoints that spanned the allowable flow range at or near rated power for all nine of the cycles studied. Therefore, the impact of operating at these lower flow conditions is included in the response to RAI 25. The three important parameters analyzed by comparison of the core tracking data to measured data; namely the hot critical eigenvalues, cold critical eigenvalues, and the TIP RMS differences, were all evaluated to see if they were sensitive the operation at high void fractions. The conclusions were that [[

]]

It was also shown in the discussion pertaining to Figure 25-10, that the exit void fractions of the low power/low flow off-rated conditions are bounded by those found at the low end of the allowable flow range at or near rated power. Also, operation at these off-rated points is generally of short duration, so the core receives very little of its total exposure accumulation at these points. Thus, the impact of higher voiding can be effectively studied by considering operation within the allowable flow range at or near rated power, which are the statepoints found in the exposure accounting. Therefore, it is concluded that the most pertinent operational data for

evaluating the fidelity of the lattice physics and core simulator codes relative to EPU/MELLLA+ operation has been included in the analyses reported in RAI 25.

RAI 26 has also requested evaluation of plant maneuvers such as reactor startup. As stated in the conclusions of the previous paragraph, GE believes that the examination of operation within the allowable flow range at or near rated power provides the pertinent operational data, and reactor startups and other off-rated maneuvers will not generate any additional insight into the methods applicability for EPU/MELLLA+, or the viability of the interim process.

NRC RAI 27

Hot Channels: The high-powered bundles are the most limiting. The core follow data is based on statistically averaged values that may not reflect how well the codes predict the conditions in the high-powered bundles. The code-to-code benchmarking using MCNP (MCNP not benchmarked with exposure and not a depletion code) may not be suitable for establishing the uncertainties and biases with depletion. In addition, the core follow TIP readings average out the four-bundle TIP readings axially within the bundle, along with all the TIP readings for a given cycle state point. In some cases, the TIP readings for different cycle points and different sets of core follow data are statistically averaged to determine the uncertainties of the core simulator codes. This approach tends to mask the accuracy of the codes in predicting hot bundle radial and axial power distribution.

Using limiting control cell loading pattern (two or three hot bundles in a control cell), benchmark the accuracy of TGBLA and PANAC in predicting the four-bundle radial and axial power distribution. Include the EPU/MELLLA+ data for the pilot plants (Brunswick Units 1 and 2 and Clinton) in your hot channel data. Provide the corresponding calculated void distribution for the hot channels.

GE Response to RAI 27

It is requested that the measured and calculated TIP readings surrounding limiting bundle locations be examined in more detailed so as to exclude effects of statistical averaging on the comparisons using plant instrumentation. To evaluate the available data, a consistent definition of what constitutes the limiting bundle needs to be made. The most limiting bundle in terms of assessing methods performance varies depending on the aspect of the methods being assessed. The limiting bundle within a core at any given point in the cycle may be that bundle closest to one of its thermal limits. Since operational performance of the bundle and the thermal limits are a function of exposure, the proximity of the bundle to its limit may not be for the highest power bundle, but may be, for instance, a moderately powered bundle at high exposures that is approaching the thermal mechanical limits curve. So too, the CPR of a bundle is a balance between the power, flow and local pin power peaking distribution within the bundle.

The limiting bundle may also be thought of as that bundle which is most challenging for the nuclear methods. Once again, depending on the aspect of the nuclear methods being examined, various parameters would result in different bundles being designated for more detailed study. High power, high void fractions, high axial peaking and steep flux gradients all contribute challenges to steady-state nuclear method fidelity. And simply, the highest power bundle may be thought of as the most limiting.

For the purposes of responding to this RAI, the highest power bundles that neighbor a TIP location are chosen for more detailed evaluation. This approach will often, while not necessarily

always, yield the best candidates for detailed "drilling down" into the substantial amount of information that is derived from in-core instrumentation.

While this detailed comparison is not consistent with the way in which the benchmarking is used in safety limit evaluations, the investigation of potential effects that the hot channel may have on TIP predictions relative to the core-wide performance is of interest for assessing the fidelity of the coupled set of steady-state nuclear methods. This prediction of in-core measurements can be evaluated throughout the exposure history of a bundle and without the operational restrictions necessary for adequate ex-core, post-irradiation measurement interpretation (such as gamma scans).

The following figures and tables provide the information requested which demonstrate a significant amount of experience for high void conditions and power profiles comparable to MELLLA+. These data are the off-line calculated instrument readings compared to the measured instrument readings from the plant. The power and void fraction data associated with these figures and tables are from the off-line calculations using TGBLA and PANAC. Plants A, B, C, D, and E are typically high power density MELLLA plants or EPU/MELLLA plants (EPU/ELLLA in the case of Plant C) for which GE/GNF has extensive operational experience. These are the same plants and plant designations for which operational experience was provided in response to RAI 25. Plant F is similar to Plant D. The specific parameters are given later in this response immediately before the TIP results for this plant are presented. For each plant cycle, the following information is provided for one or more points in each cycle.

1. For each cycle, a summary figure presents the TIP radial, axial and nodal core average RMS differences between calculated and measured TIPs. In addition, the summary figure indicates the radial difference and the axial and nodal RMS values for the TIP instrument that is adjacent to the hot channel. In this case, the "hot channel" is defined as the instrumented location with the highest power bundle of bundles surrounding instrumented locations. Cycle points where more detailed data is provided are also indicated.

   The definitions of the radial, axial and nodal statistical comparisons are provided in the response to RAI 21-2. That response includes the equations, parameter description and calculational procedure for the development of the values shown in the figures and tables below.

2. For each selected cycle exposure point (noted as 'B' for BOC, 'M' for MOC, or 'E' for EOC), a map by TIP string of the radial and axial TIP RMS difference across the core is provided. If the TIP instrument is "Failed", the TIP string was declared non-operational by the plant process computer and may be ignored. The failed TIP strings are identified in these maps by the use of asterisks next to the numbers for the TIP statistics. A lined border around a TIP statistic indicates the four-bundle grouping surrounding the TIP instrument that

corresponds to the hot channel. The four bundle cells shaded in blue represent the TIP strings that define the line of symmetry for the instrumentation strings.

3. For each cycle exposure point selected for more detailed study, a four-bundle relative power map is provided for all four-bundle cells surrounding an instrumented location. A lined border around a four-bundle power value indicates the four-bundle grouping surrounding the TIP instrument that corresponds to the hot channel. The relative power for a single bundle is normalized such that the bundle at the average bundle power has a relative power value of 1.0. The four bundle relative power is the sum of the relative powers for the four bundles in the cell.

4. For each cycle exposure point selected for more detailed study, a plot of each measured and calculated TIP instrument reading as a function of axial height is provided. The TIP plots are arranged on a core-wide map to give the relative position of the TIP within the core.

5. For each cycle exposure point selected for more detailed study, a numerical table with the nodal powers, exposures and void fractions corresponding to the four bundles surrounding the instrument adjacent to the hot channel is provided.

These tables and figures give an overview of individual TIP string statistical results for a variety of plants, cycle exposure and operating conditions. A more detailed evaluation of individual TIP string responses, errors and trending at the nodal level is given in response to RAI 29.

PLANT A CYCLE 18

Figure 27 - 1 Plant A Cycle 18 TIP Comparison Data as a Function of Cycle Exposure

[[

]]

Figure 27- 2 Plant A Cycle 18 Four Bundle Powers and TIP String Comparisons at Cycle Exposure Point B

[[

]]

Figure 27-3 Plant A Cycle 18 TIP String Comparisons at Cycle Exposure Point B

[[

]]

Table 27- 1 Plant A Cycle 18 Four Bundle Nodal Power and Void Fraction Comparisons for Hot Channel Instrument [String 16] at Cycle Exposure Point B

[[

]]

Figure 27- 4 Plant A Cycle 18 Four Bundle Powers and TIP String Comparisons at Cycle Exposure Point M

[[

]]

Figure 27- 5 Plant A Cycle 18 TIP String Comparisons at Cycle Exposure Point M

[[

]]

Table 27- 2 Plant A Cycle 18 Four Bundle Nodal Power and Void Fraction Comparisons for Hot Channel Instrument [String 16] at Cycle Exposure Point M

[[

]]

PLANT A CYCLE 19

Figure 27- 6 Plant A Cycle 19 TIP Comparison Data as a Function of Cycle Exposure

[[

]]

Figure 27- 7 Plant A Cycle 19 Four Bundle Powers and TIP String Comparisons at Cycle Exposure Point B

[[

]]

Figure 27- 8 Plant A Cycle 19 TIP String Comparisons at Cycle Exposure Point B

[[

]]

Table 27- 3 Plant A Cycle 19 Four Bundle Nodal Power and Void Fraction Comparisons for Hot Channel Instrument [String 12] at Cycle Exposure Point B

[[

]]

Figure 27- 9 Plant A Cycle 19 Four Bundle Powers and TIP String Comparisons at Cycle Exposure Point M

[[

]]

Figure 27- 10 Plant A Cycle 19 TIP String Comparisons at Cycle Exposure Point M

[[

]]

Table 27- 4 Plant A Cycle 19 Four Bundle Nodal Power and Void Fraction Comparisons for Hot Channel Instrument [String 8] at Cycle Exposure Point M

[[

]]

Figure 27- 11 Plant A Cycle 19 Four Bundle Powers and TIP String Comparisons at Cycle Exposure Point E

[[

]]

Figure 27- 12 Plant A Cycle 19 TIP String Comparisons at Cycle Exposure Point E

[[

]]

Table 27- 5 Plant A Cycle 19 Four Bundle Nodal Power and Void Fraction Comparisons for Hot Channel Instrument [String 12] at Cycle Exposure Point E

[[

]]

PLANT B CYCLE9

During the middle of the cycle, a number of TIPs for Plant B Cycle 9 were failed. The failed TIPs, which were so marked by the plant process computer, included many of the hot channels. For this comparison, a cycle exposure point after these failures had been remedied is chosen for more detailed study.

Figure 27- 13 Plant B Cycle 9 TIP Comparison Data as a Function of Cycle Exposure

[[

]]

Figure 27- 14 Plant B Cycle 9 Four Bundle Powers and TIP String Comparisons at Cycle Exposure Point B

[[

]]

Figure 27- 15 Plant B Cycle 9 TIP String Comparisons at Cycle Exposure Point B

[[

]]

Table 27- 6 Plant B Cycle 9 Four Bundle Nodal Power and Void Fraction Comparisons for Hot Channel Instrument [String 21] at Cycle Exposure Point B

[[

]]

Figure 27- 16 Plant B Cycle 9 Four Bundle Powers and TIP String Comparisons at Cycle Exposure Point M

[[

]]

Figure 27- 17 Plant B Cycle 9 TIP String Comparisons at Cycle Exposure Point M

[[

]]

Table 27- 7 Plant B Cycle 9 Four Bundle Nodal Power and Void Fraction Comparisons for Hot Channel Instrument [String 15] at Cycle Exposure Point M

[[

]]

Figure 27- 18 Plant B Cycle 9 Four Bundle Powers and TIP String Comparisons at Cycle Exposure Point E

[[

]]

Figure 27- 19 Plant B Cycle 9 TIP String Comparisons at Cycle Exposure Point E

[[

]]

Table 27- 8 Plant B Cycle 9 Four Bundle Nodal Power and Void Fraction Comparisons for Hot Channel Instrument [String 20] at Cycle Exposure Point E

[[

]]

PLANT B CYCLE 10

Figure 27- 20 Plant B Cycle 10 TIP Comparison Data as a Function of Cycle Exposure

[[

]]

Figure 27- 21 Plant B Cycle 10 Four Bundle Powers and TIP String Comparisons at Cycle Exposure Point B

[[

]]

Figure 27- 22 Plant B Cycle10 TIP String Comparisons at Cycle Exposure Point B

[[

]]

Table 27- 9 Plant B Cycle 10 Four Bundle Nodal Power and Void Fraction Comparisons for Hot Channel Instrument [String 9] at Cycle Exposure Point B

[[

]]

Figure 27- 23 Plant B Cycle 10 Four Bundle Powers and TIP String Comparisons at Cycle Exposure Point M

[[

]]

Figure 27- 24 Plant B Cycle10 TIP String Comparisons at Cycle Exposure Point M

[[

]]

Table 27- 10 Plant B Cycle 10 Four Bundle Nodal Power and Void Fraction Comparisons for Hot Channel Instrument [String 21] at Cycle Exposure Point M

[[

]]

Figure 27- 25 Plant B Cycle 10 Four Bundle Powers and TIP String Comparisons at Cycle Exposure Point E

[[

]]

Figure 27- 26 Plant B Cycle10 TIP String Comparisons at Cycle Exposure Point E

[[

]]

Table 27- 11 Plant B Cycle 10 Four Bundle Nodal Power and Void Fraction Comparisons for Hot Channel Instrument [String 24] at Cycle Exposure Point E

[[

]]

PLANT C CYCLE 30

Figure 27- 27 Plant C Cycle 30 TIP Comparison Data as a Function of Cycle Exposure

[[

]]

Figure 27- 28 Plant C Cycle 30 Four Bundle Powers and TIP String Comparisons at Cycle Exposure Point B

[[

]]

Figure 27- 29 Plant C Cycle 30 TIP String Comparisons at Cycle Exposure Point B

[[

]]

Table 27- 12 Plant C Cycle 30 Four Bundle Nodal Power and Void Fraction Comparisons for Hot Channel Instrument [String 9] at Cycle Exposure Point B

[[

]]

Figure 27- 30 Plant C Cycle 30 Four Bundle Powers and TIP String Comparisons at Cycle Exposure Point M

[[

]]

Figure 27- 31 Plant C Cycle 30 TIP String Comparisons at Cycle Exposure Point M

[[

]]

Table 27- 13 Plant C Cycle 30 Four Bundle Nodal Power and Void Fraction Comparisons for Hot Channel Instrument [String 5] at Cycle Exposure Point M

[[

]]

Figure 27- 32 Plant C Cycle 30 Four Bundle Powers and TIP String Comparisons at Cycle Exposure Point E

[[

]]

Figure 27- 33 Plant C Cycle 30 TIP String Comparisons at Cycle Exposure Point E

[[

]]

Table 27- 14 Plant C Cycle 30 Four Bundle Nodal Power and Void Fraction Comparisons for Hot Channel Instrument [String 8] at Cycle Exposure Point E

[[

]]

PLANT C CYCLE 31

Figure 27- 34 Plant C Cycle 31 TIP Comparison Data as a Function of Cycle Exposure

[[

]]

Figure 27- 35 Plant C Cycle 31 Four Bundle Powers and TIP String Comparisons at Cycle Exposure Point B

[[

]]

Figure 27- 36 Plant C Cycle 31 TIP String Comparisons at Cycle Exposure Point B

[[

]]

Table 27- 15 Plant C Cycle 31 Four Bundle Nodal Power and Void Fraction Comparisons for Hot Channel Instrument [String 9] at Cycle Exposure Point B

[[

]]

Figure 27- 37 Plant C Cycle 31 Four Bundle Powers and TIP String Comparisons at Cycle Exposure Point M

[[

]]

Figure 27- 38 Plant C Cycle 31 TIP String Comparisons at Cycle Exposure Point M

[[

]]

Table 27- 16 Plant C Cycle 31 Four Bundle Nodal Power and Void Fraction Comparisons for Hot Channel Instrument [String 11] at Cycle Exposure Point M

[[

]]

Figure 27- 39 Plant C Cycle 31 Four Bundle Powers and TIP String Comparisons at Cycle Exposure Point E

[[

]]

Figure 27- 40 Plant C Cycle 31 TIP String Comparisons at Cycle Exposure Point E

[[

]]

Table 27- 17 Plant C Cycle 31 Four Bundle Nodal Power and Void Fraction Comparisons for Hot Channel Instrument [String 8] at Cycle Exposure Point E

[[

]]

PLANT D CYCLE 13

Figure 27- 41 Plant D Cycle 13 TIP Comparison Data as a Function of Cycle Exposure

[[

]]

Figure 27- 42 Plant D Cycle 13 Four Bundle Powers and TIP String Comparisons at Cycle Exposure Point B

[[

]]

Figure 27- 43 Plant D Cycle 13 TIP String Comparisons at Cycle Exposure Point B

[[

]]

Table 27- 18 Plant C Cycle 30 Four Bundle Nodal Power and Void Fraction Comparisons for Hot Channel Instrument [String 24] at Cycle Exposure Point B

[[

]]

Figure 27- 44 Plant D Cycle 13 Four Bundle Powers and TIP String Comparisons at Cycle Exposure Point M

[[

]]

Figure 27- 45 Plant D Cycle 13 TIP String Comparisons at Cycle Exposure Point M

[[

]]

Table 27- 19 Plant D Cycle 13 Four Bundle Nodal Power and Void Fraction Comparisons for Hot Channel Instrument [String 23] at Cycle Exposure Point M

[[

]]

Figure 27- 46 Plant D Cycle 13 Four Bundle Powers and TIP String Comparisons at Cycle Exposure Point E

[[

]]

Figure 27- 47 Plant D Cycle 13 TIP String Comparisons at Cycle Exposure Point E

[[

]]

Table 27- 20 Plant D Cycle 13 Four Bundle Nodal Power and Void Fraction Comparisons for Hot Channel Instrument [String 25] at Cycle Exposure Point E

[[

]]

PLANT D CYCLE 14

Figure 27- 48 Plant D Cycle 14 TIP Comparison Data as a Function of Cycle Exposure

[[

]]

Figure 27- 49 Plant D Cycle 14 Four Bundle Powers and TIP String Comparisons at Cycle Exposure Point B

[[

]]

Figure 27- 50 Plant D Cycle 14 TIP String Comparisons at Cycle Exposure Point B

[[

]]

Table 27- 21 Plant D Cycle 14 Four Bundle Nodal Power and Void Fraction Comparisons for Hot Channel Instrument [String 11] at Cycle Exposure Point B

[[

]]

Figure 27- 51 Plant D Cycle 14 Four Bundle Powers and TIP String Comparisons at Cycle Exposure Point M

[[

]]

Figure 27- 52 Plant D Cycle 14 TIP String Comparisons at Cycle Exposure Point M

[[

]]

Table 27- 22 Plant D Cycle 14 Four Bundle Nodal Power and Void Fraction Comparisons for Hot Channel Instrument [String 11] at Cycle Exposure Point M

[[

]]

Figure 27- 53 Plant D Cycle 14 Four Bundle Powers and TIP String Comparisons at Cycle Exposure Point E

[[

]]

Figure 27- 54 Plant D Cycle 14 TIP String Comparisons at Cycle Exposure Point E

[[

]]

Table 27- 23 Plant D Cycle 14 Four Bundle Nodal Power and Void Fraction Comparisons for Hot Channel Instrument [String 14] at Cycle Exposure Point E

[[

]]

PLANT E CYCLE 9

Figure 27- 55 Plant E Cycle 9 TIP Comparison Data as a Function of Cycle Exposure

[[

]]

Figure 27- 56 Plant E Cycle 9 Four Bundle Powers and TIP String Comparisons at Cycle Exposure Point B

[[

]]

Figure 27- 57 Plant E Cycle 9 TIP String Comparisons at Cycle Exposure Point B

[[

]]

Table 27- 24 Plant E Cycle 9 Four Bundle Nodal Power and Void Fraction Comparisons for Hot Channel Instrument [String 19] at Cycle Exposure Point B

[[

]]

Figure 27- 58 Plant E Cycle 9 Four Bundle Powers and TIP String Comparisons at Cycle Exposure Point M

[[

]]

Figure 27- 59 Plant E Cycle 9 TIP String Comparisons at Cycle Exposure Point M

[[

]]

Table 27- 25 Plant E Cycle 9 Four Bundle Nodal Power and Void Fraction Comparisons for Hot Channel Instrument [String 8] at Cycle Exposure Point M

[[

]]

Figure 27- 60 Plant E Cycle 9 Four Bundle Powers and TIP String Comparisons at Cycle Exposure Point E

[[

]]

Figure 27- 61 Plant E Cycle 9 TIP String Comparisons at Cycle Exposure Point E

[[

]]

Table 27- 26 Plant E Cycle 9 Four Bundle Nodal Power and Void Fraction Comparisons for Hot Channel Instrument [String 9] at Cycle Exposure Point E

[[

]]

PLANT E CYCLE 10

Figure 27- 62 Plant E Cycle 10 TIP Comparison Data as a Function of Cycle Exposure

[[

]]

Figure 27- 63 Plant E Cycle 10 Four Bundle Powers and TIP String Comparisons at Cycle Exposure Point B

[[

]]

Figure 27- 64 Plant E Cycle 10 TIP String Comparisons at Cycle Exposure Point B

[[

]]

Table 27- 27 Plant E Cycle 10 Four Bundle Nodal Power and Void Fraction Comparisons for Hot Channel Instrument [String 12] at Cycle Exposure Point B

[[

]]

Figure 27- 65 Plant E Cycle 10 Four Bundle Powers and TIP String Comparisons at Cycle Exposure Point M

[[

]]

Figure 27- 66 Plant E Cycle 10 TIP String Comparisons at Cycle Exposure Point M

[[

]]

Table 27- 28 Plant E Cycle 10 Four Bundle Nodal Power and Void Fraction Comparisons for Hot Channel Instrument [String 18] at Cycle Exposure Point M

[[

]]

Figure 27- 67 Plant E Cycle 10 Four Bundle Powers and TIP String Comparisons at Cycle Exposure Point E

[[

]]

Figure 27- 68 Plant E Cycle 10 TIP String Comparisons at Cycle Exposure Point E

[[

]]

Table 27- 29 Plant E Cycle 10 Four Bundle Nodal Power and Void Fraction Comparisons for Hot Channel Instrument [String 13] at Cycle Exposure Point E

[[

]]

PLANT F CYCLE 15

Plant F is a target plant for MELLLA+ application. GE/GNF does not routinely receive regular TIP data from this plant. However, TIP data for three exposure points in cycle 15 are available and presented below. This plant is similar to Plant D. Specific parameters for the core are:

Plant	GE BWR Type	Number of Bundles	Original Licensed Thermal Power (OLTP) MWt	Rated Flow (Flow at OLTP) Mlbm/hr	Licensed Power Uprate (PU) % OLTP	Licensed Core Flow Range at PU % Rated Flow	Power Density at Licensed PU kW/l
F	BWR/4	560	2436	77.0	120	99-105	59.0

Figure 27- 69 Plant F Cycle 15 TIP Comparison Data as a Function of Cycle Exposure

[[

]]

Figure 27- 70 Plant F Cycle 15 Four Bundle Powers and TIP String Comparisons at Cycle Exposure Point B

[[

]]

Figure 27- 71 Plant F Cycle 15 TIP String Comparisons at Cycle Exposure Point B

[[

]]

Table 27- 30 Plant F Cycle 15 Four Bundle Nodal Power and Void Fraction Comparisons for Hot Channel Instrument [String 18] at Cycle Exposure Point B

[[

]]

Figure 27- 72 Plant F Cycle 15 Four Bundle Powers and TIP String Comparisons at Cycle Exposure Point E

[[

]]

Figure 27- 73 Plant F Cycle 15 TIP String Comparisons at Cycle Exposure Point E

[[

]]

Table 27- 31 Plant F Cycle 15 Four Bundle Nodal Power and Void Fraction Comparisons for Hot Channel Instrument [String 22] at Cycle Exposure Point E

[[

]]

PLANT F CYCLE 16

For Plant F cycle 16, TIP data for only one point is available to GE/GNF. This is at a cycle exposure of 8942 MWd/st, which corresponds to a middle of cycle point. Since only one exposure point is available, no cycle summary chart throughout the cycle is presented. Instead, the data are listed in Table 27-32.

Table 27- 32 Plant F Cycle 16 TIP Comparison Data

CYC EXP Mad/ST	Bundle RMS	Axial RMS	Nodal RMS	Max string Radial RMS	Max String axial RMS	Max String nodal RMS
8492.	[[					]]

Figure 27- 74 Plant F Cycle 16 Four Bundle Powers and TIP String Comparisons at a Cycle Exposure of 8942 MWd/st

[[

]]

Figure 27- 75 Plant F Cycle 16 TIP String Comparisons at Cycle Exposure Point B

[[

]]

Table 27- 33 Plant F Cycle 16 Four Bundle Nodal Power and Void Fraction Comparisons for Hot Channel Instrument [String 17] at Cycle Exposure Point B

[[

]]

NRC RAI 29

Calculation of Nodal, Bundle, and Axial TIP Responses. RAI 29 follows up on methods RAI 21-2. The objective is to determine whether the statistical combination and normalization of the measured and the calculated TIP data comparisons show the axial and nodal differences between the calculated and the measured data for a four-bundle TIP cell.

29-1 Using a limiting four-bundle TIP cell (limiting number of hot bundles in a control cell, limiting enrichment, limiting cycle exposure point), tabulate the TIP calculated and measured data. Show how the axial, bundle, and nodal TIP RMS is calculated from the TIP readings.

29-2 For the same four-bundle TIP data, compare the absolute calculated and measured values for each TIP element reading and provide a tabulation of the corresponding bundle axial void profiles and the absolute difference in TIP data.

29-3 Evaluate the absolute difference in TIP readings and determine whether the fidelity of the TIP readings varies axially with void. Compare the four-bundle TIP data with core follow TIP readings for less challenging core and lattice designs and determine whether the four-bundle power uncertainties should be increased.

29-4 Since the four-bundle control cell can contain bundles at different exposures, explain how the accuracy of the GNF-A methods can be benchmarked for depletion under high-void conditions by using the core follow data. This issue is important because MCNP is not well-suited for benchmarking the historical effects. Use gamma scan data, if available, for bundles and peak pin at different exposures (e.g., fresh, once-burned, twice- burned). As an interim measure, select four-bundle TIP readings and cycle state points to assess the fidelity of TGBLA and PANAC for depletion at high-void conditions. State whether the accuracy of the code for the hot bundle changes with exposure at core conditions as close to EPU/MELLLA+ conditions as possible.

GE Response

Response to 29-1

To demonstrate how the bundle, axial and nodal TIP statistical values are calculated from the TIP readings, it is desirable to choose a TIP string that is limiting in the sense that it is surrounded by hot bundles with high enrichment and at a limiting point in exposure. This is necessarily a more limiting configuration than an arrangement of hot bundles in a control cell. In addition, most core configurations are not operated in control cell core configurations due to the high batch fractions.

Not all of the characteristics that result in hot bundles surrounding an instrument location are maximized at a particular exposure point in a particular cycle of a particular plant with a particular bundle arrangement at a particular TIP location, but there are a number of instances in

the previously presented data where all of these parameters are at or near their maximum. In particular, TIP string 24 of Plant B cycle 10 is surrounded by two fresh and two once-burned bundles of [[ ]] wt% and [[ ]] wt% bundle average enrichment, respectively. At the end of cycle (exposure point E in the response to RAI 27), the normalized four-bundle power is [[ ]]. For the power density of this core, that four-bundle power represents an average bundle power in the four bundles of about [[ ]]. This is the highest absolute average bundle power in any four-bundle cell in the data provided. Therefore, the hot channel TIP data from the response to RAI 27 will be used to demonstrate the TIP statistic calculations.

Table 29-1 shows the axial node of the data in the core simulator, the axial elevation in inches, the calculated TIP prediction (CALTIP), the measured TIP reading (PCTIP) and the nodal difference between the calculated TIP value and the measured TIP reading (Delta).

From the response to RAI 21-2, the radial, or bundle, statistic for a single TIP string is given by:

$$\Delta_{j,rad} = \left(\frac{\sum_{k=Klow}^{Kup} C(k,j)}{K} \right) - \left(\frac{\sum_{k=Klow}^{Kup} P(k,j)}{K} \right)$$

Each of the CALTIP and PCTIP columns is summed between the nodes of interest. As mentioned in an earlier response, instrument readings are generally of interest only in the region of nodes 2 to 23 due to end effects and instrument reading validity. Therefore, the columns are summed only over nodes 2 to 23, and the sum is divided by K, which in this case is 22. This gives a value of

$$\Delta = 1.245 - 1.263 = -0.019$$

This value results in a -1.9% radial difference. The percentage represents the difference in the axially integrated four-bundle power difference between calculated and measured expressed as a percentage of the average four-bundle (or TIP string) power.

From the response to RAI 21-2, the nodal RMS for the string is found by taking the square root of the sum of the squares in the "Delta" column (for nodes 2 to 23) divided by the number of values (again, in this case, 22). This gives a value of [[ ]]. Again, this represents the nodal RMS value in terms of an average node in the core.

As indicated in the response to RAI 21-2, the axial RMS value for a single string is obtained by first normalizing the CALTIP and PCTIP data for the string with itself and then performing the same operation used in calculating the nodal RMS. Again, only data between the nodes of interest are used. Table 29-2 shows the normalized data from Table 29-1.

The axial RMS is found by taking the square root of the sum of the squares of the "Delta" column in Table 29-2 divided by 22. This gives a value of [[ ]]. This is an indicator of the relative axial shape comparison between calculated and measured, without the overall radial magnitude in the comparison.

Response 29-2

Table 29-3 repeats the data from Table 29-1. These are the absolute calculated and measured TIP element readings for the single, "hottest" TIP instrument in this particular cycle, string 24 (see response to RAI 27). The "Delta" column in Table 29-3 is the tabulation of the absolute difference at each node. Also shown is the calculated void fraction for each node for each of the four surrounding bundles. The void fraction data may also be found in the response to RAI 27.

Response 29-3

The data from Table 29-3 are plotted in Figure 29-1. The absolute difference in TIP values shown as a function of the four bundle average void fraction reveals no correlation of the TIP difference with void fraction. The choice of average or hot channel void fraction as the abscissa does not much matter since all void fractions are roughly within 5% of one another in this particular hot channel data set. Again, the values for nodal differences are relative to the average power node in the core.

The figure does not demonstrate a correlation of TIP error with the axial variation in void fraction.

To provide context and perspective of this difference in shape, it is necessary to evaluate this TIP response relative to other TIP differences. It is instructive to look at other TIPs in the same core at the same exposure point, as well as to look at other plant cycles that have both more and less challenging conditions for TIP calculations.

Figure 29-2 shows the nodal difference between calculated and measured TIPs for Plant E Cycle 10, Exposure Point M for the instrument location that has the highest power monitored bundle. This same data may be found from the response to RAI 27.

Again, the figure does not demonstrate a correlation of TIP error with the axial variation in void fraction.

Figure 29-3 shows a similar plot for a less challenging core and lattice design. These data come from the "hottest" TIP for Plant A Cycle 18 exposure point B. Here there is a more pronounced trending with void fraction in the lower portion of the bundle, but still the majority of difference points do not have a correlation with increasing void fraction. In fact, what is being

demonstrated with these graphs is that the magnitude of the nodal difference tends to follow the magnitude of the absolute nodal power, rather than the void fraction.

To compare a variety of plants, cycle exposures and operating conditions, the nodal differences for the TIP adjacent to the highest power bundle from all the data presented in response to RAI 27 are plotted together in a single graph shown in Figure 29-4. The values are the absolute TIP nodal differences plotted versus the four bundle averaged axial void fraction for the TIP with the highest power bundle for those exposure points examined in detail in RAI 27.

The relatively even data scatter about the x-axis indicates that, even considering the limiting TIP within the core and for the limiting core designs and exposure points in the cycle, the nodal uncertainty between calculated and measured TIPs is not increasing as a result of increasing void fraction. Although the observation with axial void fraction is made using nodal differences, and the four bundle power uncertainties are defined using the RMS radial differences, it can be concluded that, lacking a void dependency on the nodal differences, the integral of those differences would also lack void dependency. Therefore, the four bundle power uncertainties do not need to be increased.

Response 29-4

In addressing this question, it is important to put the depletion history at high void concentrations in perspective. Plant E is an example of an aggressive application of power uprate, being a BWR/6 uprated to 120% of original rated power. In addition, Cycle 9, its most recent full cycle of operation, is a two-year cycle with an exposure of approximately 16000 MWD/ST. The operation history is summarized in Table 25-9 of RAI 25. Peak void fractions of 88% are common during its operation, leading one to believe that a significant amount of burnup is achieved at void fractions of 85% and above. In reality, bundles do not stay at the maximum power throughout their entire life, so the exposure weighted density, UH for the maximum power bundle in the core is representative of a void fraction less than the 88% maximum void fraction exhibited throughout the cycle. Nodes having high void fractions for the majority of their time in the core will also tend to have lower power density and hence lower burnup at the end of cycle. These trends are illustrated in Figure 29-5, where a plot of nodal UH (exposure weighted water density) is plotted vs. nodal exposure for all nodes in the Plant E core at the end of Cycle 9. This figure focuses on the high exposure, high void fraction part of the core (the values for UH below 0.6 are not shown for clarity). The values of UH corresponding to 80%, 83% and 86% voids are shown on the graph. The following observations can be noted from this Figure:

- No nodes have a void history greater than 86%, and those approaching 86% have a burnup around 5000 MWD/ST.

- About 4% of the nodes have a void history corresponding to greater than 83% and their maximum exposure is less than 20000 MWD/ST

- Less than 12% of the nodes have void histories greater than 80% voids and all have exposures less than 37000 MWD/MT. This 80% void fraction representing a significant fraction of depletion history is 8% less than the maximum fraction noted in the plant history tables.

The application presented here represents the highest probability for achieving high exposure at a high void fraction, i.e., a high power density plant with a high cycle exposure. A small portion of the bundles operates at very high voids and an even smaller portion of those burn to a high exposure.

Four bundle cells surrounding TIPs are comprised of bundles with various characteristics and at various exposures. Comparisons of the axial and radial TIP readings with calculations provide a benchmarking of the calculational methods in that these comparisons inherently contain the effects of depletion. These measurements are taken routinely throughout a cycle and provide direct and immediate feedback to the core monitoring. These readings can also be used to examine the fidelity of the nuclear methods as a function of exposure. This is in contrast to gamma scans, which are discussed in the response to RAI 28.

Specifically, one can observe a single TIP string throughout the cycle. If one chooses a TIP string, around which are loaded two fresh bundles and two once-burned bundles, then the effects of high void depletion can be observed. It should be noted that, in general, high exposure bundles are not depleted under high void conditions since these bundles are naturally lower in power later in life. Figure 29-5 demonstrates this point.

Further illustration of TIP string behavior is provided in data from Plant A Cycle 19, as shown in Figure 29-6. TIP string 12 is loaded with two once burned bundles and two fresh bundles. The radial differences for TIP string 12 as the fresh bundles deplete throughout the cycle do not rise throughout the cycle. The nodal RMS values through the cycle are not significantly different than those of the core average. Figure 29-7 shows similar data for Plant B Cycle 10. TIP string 8 is loaded with two fresh bundles and two once burned bundles. Again, the radial difference of this TIP does not exhibit an increasing trend with exposure and the nodal RMS value is not significantly different than the core average nodal RMS value.

These nodal comparisons, while not directly used in evaluations of SLMCPR or other licensing parameters, have been shown to be acceptable. Both the core average RMS difference of all nodal instrument predictions to measured TIP data and the "hot" TIP string, have an average RMS nodal difference of generally less than [[ ]] for the strings depicted in Figures 29-6 and 29-7, indicating that axial power distributions are also predicted adequately. This level of agreement is generally taken to be quite good.

Table 29- 1 TIP Data from Plant B Cycle 10, Exposure Point E, TIP string 24

Node	TIP Z (in)	CALTIP	PCTIP	Delta
24	141.0	[[		
23	135.0			
22	129.0			
21	123.0			
20	117.0			
19	111.0			
18	105.0			
17	99.0			
16	93.0			
15	87.0			
14	81.0			
13	75.0			
12	69.0			
11	63.0			
10	57.0			
9	51.0			
8	45.0			
7	39.0			
6	33.0			
5	27.0			
4	21.0			
3	15.0			
2	9.0			
1	3.0			]]

Table 29- 2 Normalized TIP Data from Plant B Cycle 10, Exposure Point E, TIP string 24 for Axial Computations

Node	TIP Z (in)	CALTIP	PCTIP	Delta
23	135.0	[[		
22	129.0			
21	123.0			
20	117.0			
19	111.0			
18	105.0			
17	99.0			
16	93.0			
15	87.0			
14	81.0			
13	75.0			
12	69.0			
11	63.0			
10	57.0			
9	51.0			
8	45.0			
7	39.0			
6	33.0			
5	27.0			
4	21.0			
3	15.0			
2	9.0			]]

Non-proprietary version

Table 29-3 Calculated and Measured TIP readings and Surrounding Bundle Void Fraction Profiles for Plant B Cycle 10 Exposure Point E TIP String 24

Axial Node	BUNDLE LOCATION (24,14) Void	(25,14) Void	(24,15) Void	(25,15) Void	CALTIP	PCTIP	Delta
25	[[						
24							
23							
22							
21							
20							
19							
18							
17							
16							
15							
14							
13							
12							
11							
10							
9							
8							
7							
6							
5							
4							
3							
2							
1							]]

Figure 29-1 Difference Between Calculated and Measured TIP Readings As a Function of Surrounding Bundle Void Fraction for Plant B Cycle 10 Exposure Point E TIP String 24

[[

]]

Figure 29-2 Difference Between Calculated and Measured TIP Readings As a Function of Surrounding Bundle Void Fraction for Plant E Cycle 10 Exposure Point M TIP String 18

[[

]]

Figure 29-3 Difference Between Calculated and Measured TIP Readings As a Function of Surrounding Bundle Void Fraction for Plant A Cycle 18 Exposure Point B TIP String 16

[[

]]

Figure 29-4 Absolute Nodal Differences Between Calculated and Measured TIP Readings As a Function of Surrounding Bundle Void Fraction

[[

]]

Figure 29-5 Nodal Void History as a Function of End of Cycle Nodal Exposure for Plant E, Cycle 9

[[

]]

Figure 29-6 Nodal and Radial Differences Between Calculated and Measured TIP Readings for Plant A Cycle 19 TIP String 12 As a Function of Cycle Exposure

[[

]]

Figure 29-7 Nodal and Radial Differences Between Calculated and Measured TIP Readings for Plant B Cycle 10 TIP String 8 As a Function of Cycle Exposure

[[

]]